Schwinger Pair Production at Finite Temperature and Novel Astrophysical Probes on Millicharged Fermions

A Thesis

submitted to
Indian Institute of Science Education and Research Pune
in partial fulfillment of the requirements for the
BS-MS Dual Degree Programme

by

Mrunal Prashant Korwar

IISER PUNE

Indian Institute of Science Education and Research Pune
Dr. Homi Bhabha Road,
Pashan, Pune 411008, INDIA.

May, 2018

Supervisor: Dr. Arun Thalapillil

Certificate

This is to certify that this dissertation entitled Schwinger Pair Production at Finite Temperature and Novel Astrophysical Probes on Millicharged Fermions towards the partial fulfilment of the BS-MS dual degree programme at the Indian Institute of Science Education and Research, Pune represents study/work carried out by Mrunal Prashant Korwar at Indian Institute of Science Education and Research under the supervision of Dr. Arun Thalapillil, Assistant Professor, Department of Physics , during the academic year 2017-2018.

Dr. Arun Thalapillil

Committee:

Dr. Arun Thalapillil

Dr. Prasad Subramanian

This thesis is dedicated to friends and family

Declaration

I hereby declare that the matter embodied in the report entitled Schwinger Pair Production at Finite Temperature and Novel Astrophysical Probes on Millicharged Fermions are the results of the work carried out by me at the Department of Physics, Indian Institute of Science Education and Research, Pune, under the supervision of Dr. Arun Thalapillil and the same has not been submitted elsewhere for any other degree.

Mrunal Prashant Korwar

Acknowledgments

I would like to express my sinceare gratitude to my theis advisor Dr. Arun Thalapillil, for help, guidance and support. Apart from physics, I learned from him to identify essence and cavetes in the reseacrh project and to put off biases and be an independent thinker. I would like thank my TAC memeber Dr. Prasad Subramanian for aggreeing to be one of the mentors in thesis advisory comitee and evaluating my mid-year report, presentaion and final thesis. I would also like to thank the Physics department for providing resources required for the project work. I thank Dr. Sunil Mukhi, Dr. Namabita Banerjee and Dr. Sachin Jain for the weekly string theory club discussions. I also sincerely extend my gratitude towards the KVPY (by the Department of Science and Technology, Government of India), for providing financial support throughout my study at IISER Pune. I would like to thank Dr. Anson Hook for helpful discussions. I would like to thank my freinds and family for their constant support throughout this project.

Abstract

Schwinger pair production is a non-perturbative and non-linear phenomenon in Quantum Electroynamics. It is equally interesting to theoretical and experimental physics because of the necessity of strong electric field required to study it. Many theoretical models have been developed to explain and extend the result for number of pair produced from Scalar QED and QED vacuum. We use Worldline Instanton method to find vacuum decay rate for scalar QED and QED vacuum in presence of constant Electric field and constant Electric field parallel to Magnetic field at zero temperature in weak field aprroximation and weak coupling limit. We thus verify results obtained by other theoretical methods for these field configurations. We extend the result to finite temperature case i.e. we give an analytical expression for Scalar QED and QED vacuum decay rate in presence of constant Electric field and constant Electric field parallel to magnetic field at some non-zero temperature in weak field approximation and weak coupling limit.

Schwinger pair production of electron-positron pairs requires constant electric field of the order of $10^{18} V/m$. This huge electric field is not achieved in laboratory till now. Some of the astronomical objects like Magnetars do produce electric field of the order of $10^{14} V/m$. Many extensions of the standard model generically give rise to hypothetical Millicharged particles. These are particles with fractional electric charges. Millicharged particles are intersting from the viewpoint of charge quantization and they are viable dark matter candidate too.

Schwinger pair production of Millicharged particle is possible in the Magnetar environment and affect the magnetic field evolution of magnetar. We provide novel, model independent constraints on these hypothetical particles based on Energy loss argument and Magnetic field evolution argument. We also show the effect of millicharged particles on the braking index of the magnetar.

Contents

List of Figures

Chapter 1

Introduction

1.1 Introduction to Schwinger Pair Production

The Phenomenon of pair production from vacuum in presence of constant Electric field (termed as "Schwinger Pair Production") was first proposed by Euler and Heisenberg [1] and later formulated in the modern language of Quantum Field theory by Schwinger [2] (see [3] about related historical facts). The rate at zero temperature had the $O(\exp(-\pi m^2/eE))$ behavior showing the non-perturbative nature of the process and necessity of Strong Electric field $O(10^{18})V/m$ for the observation of Phenomenon. Because of both theoretical (relating to non-perturbative character) and Phenomenological (probing at strong fields) interest it has applications in many areas of physics [4][5][6][7]. Reaching such a high electric field is an experimental challenge. Therefore there have been several studies regarding the experimental verification of Schwinger effect (see [8][9] for reviews). Although the strength of electric field required is still not reached, but it will be accessible to some of the upcoming laser facilities like Extreme Light Infrastructure (ELI) and European X-ray Free Electron Laser (European XFEL).

In order to study pair production in external field various theoretical methods have been developed - Schwinger's proper time method [2], WKB technique[10], Schrödinger-Functional approach[11], functional techniques[12][13], kinetic equations[14][15], various instanton techniques[16][17], Borel summation [18], Worldline numerics[19], and evolution operator method [20].

The result of vacuum decay rate in presence of constant Electromagnetic field has been extended to Finite Temperature as well. QED effective action at finite temperature in presence of constant Magnetic field has been found first by Dittrich[21]. Since then this has motivated the study of QED and SQED at finite temperature under various configurations of electromagnetic fields and thereby the Schwinger pair production at finite temperature, which has been an issue of debate depending on formalisms employed[22][23][24][11][25]. The issue was resolved by evolution operator formalism by finding non-zero thermal correction to zero temperature vacuum decay rate at one-loop level in constant Electric field[26]. Recently, Worldline Instanton formalism has been used to calculate analytical expression for the vacuum decay rate in constant Electric field for Scalar particles at finite temperature which is also extended to arbitrary coupling in weak external fields[27][28].

The Worldline formalism has been very powerful tool for quantum field theory both at one-loop and higher loop which was used in [29][30] to calculate gauge theory amplitudes. Naturally, the Worldline formalism has been used to reproduce and extend Schwinger's result both at zero temperature[31][16][32] for scalar particles in presence of constant Electric background and finite temperature for scalars in constant electric background[27] and also at arbitrary coupling [28]. We extend the Worldline formalism method to calculate Vacuum decay rate for both Scalar and Spinor in presence of constant Electric field parallel to Magnetic Field at zero temperature thus deriving results already known in the literature [17]. We extend the result to finite temperature for both Scalars and Spinor in presence constant $\boldsymbol{E}$ and constant $\boldsymbol{E} \parallel \boldsymbol{B}$ field thus verifying the result of [27] for scalar pure $\boldsymbol{E}$ case.

1.2 Introduction to Dark Matter Physics

The standard model of particle physics has been a most successful theory whose predictions have been tested experimentally with good precision. Nevertheless, it is incomplete as it can not explain presence of dark energy, dark matter, neutrino masses and matter-antimatter asymmetry. A good amount of observational data from astrophysics and cosmology suggests gravitational interaction between Baryonic matter and non-luminous matter. Nature of this "Dark Matter" is unknown. It is natural to believe that the new particles that could account for dark matter appear in various theories beyond standard model of particle physics. The identification of the nature of the dark matter would answer one of the most important open question in physics and would help to better understand universe and its evolution.

The first hint for presence of dark matter came from Fritz Zwicky[33]. He observed unexpectedly high velocities of nebulae in the coma cluster which brought him to the idea of dark matter. In 1978, Rubin et al.[34] found that rotation velocities of stars in galaxies stay constant with increasing distance from galactic centers. This was contradictory to the expectation from Newtonian dynamics, according to which rotation velocities should fall as distance increases from galactic center. This problem was resolved by the work of Ostriker and Peebles [35] who suggested the presence of Dark Matter halo to explain instabilities in the models of galactic disk. In recent times, x-ray spectroscopy of hot gas in elliptical galaxies[36] and gravitational lensing [37] provides the confirmation of dark matter hypothesis. Further evidence for the dark matter comes from cosmology as it is required to generate density perturbations that led to large scale structures [38] and to account for big-bang nucleosynthesis [39].

In order to account for above astrophysical observations, modified Newtonian dynamics model (MOND) [40] and its relativistic extension TeVes [41] were proposed. Though these solutions correctly described the rotational velocities measured in galaxies but failed to describe large scale structure and CMB structure correctly[42]. Massive astrophysical compact halo object (MACHOs) - an astrophysical objects that would emit very less or no radiation were also thought of as possible explanation of dark matter. Searches for these objects using gravitational micro-lensing have been performed[43] showing they could account for at most 20 percent of dark matter in our galaxy. A model with MACHOs accounting for all the dark matter were also ruled out [44]. Primordial black holes as an explanation for dark matter abundance was also considered[45][46].

It was also thought that dark matter is made out of massive neutral particle with weak self interaction. Sterile neutrinos were thought to be such a viable dark matter candidate [47][48]. This particles were constrained by x-ray measurements and viable only in the keV range. Because of their low mass and interaction strength they can not be probed by direct detection experiment. Models beyond standard model of particle physics suggested a viable dark matter candidate which is stable, neutral and have mass in the range from GeV to several TeV. This particles are termed as Weakly Interacting Massive Particle (WIMP). These particles could account for right relic abundance of dark matter in universe[49]. Despite their experimental searches no unambiguous signal of their presence has been confirmed. The neutralino from Supersymmetry models and 'light Kaluza particles' from models in extra dimension are particles fulfilling properties of WIMP(see [50] for review on WIMP and current bounds). 'Superheavy dark matter' are possible 'non-WIMP' dark matter candidate proposed in order to explain the origin of ultra-high energy cosmic rays[51][52].

Weakly interacting sub-eV particles (WISP) are the viable dark matter candidates with mass ranging from sub-femto-eV to hundreds of GeV. Axions, Axion like Particles (ALPs), Milli-charged particles, hidden sector photons, chameleons, and other related particles are particles under WISP category[53]. Axions are pseudo-scalar particles that solve strong CP problem. They are pseudo-nambu goldstone bosons of Pecci-Quinn symmetry. They are light and have possible couplings with photon, gluons and standard model fermions. Hidden sector photons A' photons are massive vector bosons coupled to ordinary photon with kinetic mixing. Sub-eV dark photon could be viable dark matter candidate (See [54] for current bounds and experimental probes). It is possible to have dark matter to be part of hidden sector and couple to an A'. A hidden sector coupled to massless A' will give rise to millicharged particle which can be a viable dark matter candidate[53].

In chapter 4 we will review one-para-photon model, along with some of the present constraints on millicharged particles. We will also review how some of the stringent constraints can be evaded with Two para-photon model. Milli-charged particles arise in the large class of standard model extension[55][56][57][58][59]. They have been studied in the context of observational anomalies[60]. Since millicharged particles can have fractional charges hence they are intriguing from the viewpoint of charge quantization. In chapter 5 we'll give a brief introduction to Neutron stars and Magnetars and will provide novel constraints based on energy-loss argument and magnetic field evolution argument. We will also show the effect of Millicharged particles on the braking index of neutron star.

Chapter 2

Schwinger Pair Production in Scalar Electrodynamics

2.1 Zero Temperature Case

2.1.1 One Loop Effective Action

We want to calculate the pair production rate from vacuum made unstable by presence of external fields. Probability for vacuum to vacuum transition is given by $\left|\left\langle 0_{out}|0_{in}\right\rangle\right|^2$. In absence of external fields, this is unity. But, adiabatically turning on electric field will give rise to false vacuum. Thus making probability for production of particles non-zero, this will be characterized in the imaginary part of ground state energy of false vacuum. In presence of external field sourced by potential A, the probability of vacuum to vacuum transition is given by

$$\left\langle 0_{out}|0_{in}\right\rangle^A = \exp(iW^{\mathbb{M}}(A)) \tag{2.1}$$

then,

$$\begin{aligned} \text{Probability of vacuum decay} &= 1 - e^{iW^{\mathbb{M}}(A)}e^{-iW^{\mathbb{M}}(A)} \\ &= 1 - e^{2\mathrm{Im}W^{\mathbb{M}}(A)} = 2\mathrm{Im}(W^{\mathbb{M}}(A)) \end{aligned} \tag{2.2}$$

Probability of vacuum decay is number so independent of whether we calculate RHS in Minkowaskain or Euclidean co-ordinate We have in Minkowaskian time

$$e^{iW^{\mathbb{M}}} = \left\langle 0 \middle| e^{-iHT} \middle| 0 \right\rangle = \int D\phi D\phi^* e^{iS_{\mathbb{M}}} \tag{2.3}$$

converting to Euclidean time we get

$$e^{-W^{\mathbb{E}}} = \int D\phi D\phi^* e^{-S_{\mathbb{E}}} \tag{2.4}$$

Hence,

$$\text{Probability of vacuum decay} = 2\text{Im}(W^{\mathbb{M}}(A)) = 2\text{Re}(W^{\mathbb{E}}(A)) \tag{2.5}$$

Quantity of interest is probability of vacuum decay per unit space-time volume (Γ)

$$\Gamma = 2\frac{\text{Re}(W^{\mathbb{E}}(A))}{V_3 T} = 2\text{Im}\left[\frac{W^{\mathbb{E}}(A)}{V_4^{\mathbb{E}}}\right] \tag{2.6}$$

where we have assumed that external fields as well as false vacuum state is homogeneous. In presence of finite temperature, $V_4^{\mathbb{E}}$ will be replaced by $V_3\beta$ where β is equal to inverse temperature. In Euclidean metric, the relation between $W^{\mathbb{E}}$ and Scalar QED action S (where we have dropped subscript $\mathbb{E}$) is given by [61]

$$\exp(-W^{\mathbb{E}}(A)) = \int D\phi D\phi^* \exp[-S] \tag{2.7}$$

and

$$S = \int d^4x\,(\phi^*(-D^2 + m^2)\phi) + \frac{1}{4}F_{\mu\nu}^2$$

is the Euclidean action. Where $D_\mu = (\partial_\mu + ieA_\mu)$ and $A_\mu = (A_1, A_2, A_3, A_4)$ such that $A_4 = -iA_0$ (where on the Minkowaskian side we have used $(1,-1,-1,-1)$ metric convention) and other components are same as Minkowaskian A_μ. The Electromagnetic field tensor is $F_{\mu\nu} = \partial_\mu A_\nu - \partial_\nu A_\mu$. In order to arrive at given expression of Euclidean Action we have used following Lagrangian density on the Minkowaskian side:

$$\mathscr{L}^{\mathbb{M}} = (\partial_\mu - ieA_\mu)\phi^*(\partial^\mu + ieA^\mu)\phi - m^2\phi^*\phi - \frac{1}{4}F_{\mu\nu}F^{\mu\nu} \tag{2.8}$$

where μ runs from 0 to 3, when converted to Euclidean signature will look like

$$\mathscr{L}^{\mathbb{E}} = (\partial_\mu - ieA_\mu)\phi^*(\partial_\mu + ieA_\mu)\phi + m^2\phi^*\phi + \frac{1}{4}F_{\mu\nu}^2 \tag{2.9}$$

where μ runs from 1 to 4, such that $A_4 = -iA_0$. We use steepest decent approximation in RHS of eq.(2.7)

$$S[\phi,\phi^*] = S[\phi_{cl},\phi_{cl}^*] + \int \frac{\delta^2 S}{\delta\phi(x)\delta\phi^*(y)}\eta(x)\eta^*(y)d^4x d^4y \tag{2.10}$$

We have used multidimensional taylor series expansion. The factors like $\delta^2 S/\delta\phi\delta\phi$ and $\delta^2 S/\delta\phi^*\delta\phi^*$ are zero. The (ϕ_{cl},ϕ_{cl}^*) is the solution which make $\delta S/\delta\phi$ and $\delta S/\delta\phi^*$ vanish. The η and η^* are fluctuations about classical path, vanishing at the end points of path.

Using eq.(2.7) and (2.10), we get

$$\begin{aligned}\exp(-W^{\mathbb{E}}(A)) &= \int D\phi D\phi^* \exp[-S] \\ &= \exp(-S(\phi_{cl}))\int D\eta\, D\eta^* \exp\big(-\int d^4x d^4y\, \eta(x)(-D^2+m^2)\eta^*(y)\big) \\ &= (\det(-D^2+m^2))^{-1}\exp(-S(\phi_{cl}))\mathscr{N} \\ &= \exp(-\mathrm{Tr}\ln(-D^2+m^2))\exp(-S(\phi_{cl}))\mathscr{N}\end{aligned} \tag{2.11}$$

where $\mathscr{N}$ is normalization constant. We have discretized the integral in the exponent of eq.(2.11), then using the multidimensional version of Gaussian integral over complex variables

$$\int dz_1 dz_1^* \cdots dz_d dz_d^* \exp\big(-z^\dagger A z\big) = (2\pi)^d \exp(-\mathrm{tr}\ln A) \tag{2.12}$$

which assumes that A is a Hermitian operator and can be normalized by some unitary matrix. This assumption is valid for operator $(-D^2+m^2)$. From eq.(2.11) and (2.6), we write

$$2\mathrm{Im}(W^{\mathbb{E}}(A)/V_4^{\mathbb{E}}) = 2\mathrm{Im}(\mathrm{Tr}\ln(-D^2+m^2)/V_4^{\mathbb{E}}) \tag{2.13}$$

we have dropped the normalization constant $\mathscr{N}$ and $S(\phi_{cl})$ as both of these do not give any Imaginary contribution.

We use mathematical identity (Frullani's Integral) to simplify further

$$Tr(\ln(P)) = -\int_0^\infty \frac{dT}{T} Tr(\exp(-PT) - \exp(-T)) \tag{2.14}$$

Identifying P in the above expression by $-D^2+m^2$. We neglect second term in the eq.(2.14) since it does not contribute to the imaginary part. Since,

$$-\int_0^\infty \frac{dT}{T} Tr(\exp(-PT)) = -\int_0^\infty \frac{dT}{T} \int dx(\langle x|\exp(-PT)|x\rangle) \tag{2.15}$$

we can convert eq.(2.13) to [16]

$$W^{\mathbb{E}}(A) = -\int_0^\infty \frac{dT}{T} \exp[-m^2 T] \oint [dx_\mu] \exp\Big[-\int_0^T d\tau \big[\frac{1}{4}\dot{x}^2 + ieA_\mu \dot{x}^\mu\big]\Big] \tag{2.16}$$

Considering $-D^2+m^2 = -(\partial+ieA)^2+m^2$ as Hamiltonian, then the Lagrangian can be computed as follows: replace ∂ with ip then treat p as momentum variable, the Lagrangian then can be obtained by Legendre transform in terms of $\dot{x}$; replacing t with $-i\tau$, we get

$$-\left(\frac{\dot{x}^2}{4} + ieA\dot{x} + m^2\right) \tag{2.17}$$

Hence we get eq.(2.16) as the final expression for 1-loop effective action for SQED case. Where $x_\mu(\tau)$ path should satisfy the periodic boundary condition $x(0) = x(T)$.

We substitute $\tau = T\,u$,and $T \to T/m^2$ in eq.(2.16)

$$W^{\mathbb{E}}(A) = -\int_0^\infty \frac{dT}{T} \exp[-T] \oint [dx_\mu] \exp\Big[-\Big(\frac{m^2}{4T}\int_0^1 du\dot{x}^2 + ie\int_0^1 duA.\dot{x}\Big)\Big] \tag{2.18}$$

where $x_\mu(u)$ path should satisfy the periodic boundary condition $x(0) = x(1)$.

We evaluate T integral first which gives Modified Bessel function of second kind $K_0(z)$ reducing above expression to[16]

$$W^{\mathbb{E}}(A) = -2\int [dx_\mu] K_0\Big(m\big(\int_0^1 \dot{x}^2 d\tau\big)^{1/2}\Big) \exp\Big(-ie\int_0^1 duA.\dot{x}\Big) \tag{2.19}$$

Since in the limit $z >> 1$ the Modified second Bessel function behaves as

$$K_0(z) \approx \sqrt{\frac{\pi}{2m}} \exp(-z) \tag{2.20}$$

hence for the approximation $m\sqrt{\int_0^1 \dot{x}^2} >> 1$ (which corresponds to weak field limit $m^2 >> eE$) eq.(2.19) reduces to

$$W^{\mathbb{E}}(A) = -\sqrt{\frac{2\pi}{m}} \int [dx_\mu] \frac{1}{[\int_0^1 \dot{x}^2\, du]^{1/4}} \exp\left[-m\sqrt{\int_0^1 \dot{x}^2 du} - ie\int_0^1 A.\dot{x}du \right] \tag{2.21}$$

Another way to reach above equation from eq.(2.18) is to perform saddle point approximation to T integral. The saddle point is given by

$$T_0 = \frac{m}{2}\Big(\int_0^1 \dot{x}^2\, du\Big)^{1/2} \tag{2.22}$$

thus in the weak field limit we get eq.(2.21). As, according to saddle point approximation:

$$\int h(x) e^{Mg(x)} dx \approx \sqrt{\frac{2\pi}{M|g''(x_0)|}}\, h(x_0) e^{Mg(x_0)} \text{ as } M \to \infty \tag{2.23}$$

where x_0 is the saddle point.

We consider terms in the exponent of eq.(2.21) as $-S_{\text{eff}}$, the Euler-Lagrange equation is given by[62]

$$m\ddot{x}_\mu = ie\sqrt{\int_0^1 du\dot{x}^2}\; F_{\mu\nu}\dot{x}_\nu \tag{2.24}$$

Because of the antisymmetric property of $F_{\mu\nu}$ we get $\dot{x}^2$ = constant = a^2. Where $a = 2mp\pi/eE$, as we will see later, is obtained by imposing periodic boundary condition on solution of eq.(2.24). The derivation of eq.(2.24) is presented below

$$\begin{aligned}
\frac{\delta S_{\text{eff}}}{\delta x^a(p)} &= \frac{m}{2\sqrt{\int_0^1 du\dot{x}^2}}\frac{\delta(\int_0^1 du\dot{x}^2)}{\delta x^a(p)} + ie\int_0^1 \frac{\delta A_\mu(x)}{\delta x^a(p)}\dot{x}^\mu(u)du + ie\int_0^1 duA_\mu\frac{\delta\dot{x}^\mu(u)}{\delta x^a(p)} \\
&= \frac{m}{\sqrt{\int_0^1 du\dot{x}^2}}\int_0^1 du\dot{x}_\mu\frac{\delta\dot{x}^\mu(u)}{\delta x^a(p)} + ie\int_0^1 du\frac{\partial A_\mu(x(u))}{\partial x^\nu(u)}\frac{\delta x^\nu(u)}{\delta x^a(p)}\dot{x}^\mu - ie\int_0^1 du\frac{\partial A_\mu(x(u))}{\partial x^\nu(u)}\frac{\delta x^\mu(u)}{\delta x^a(p)}\dot{x}_\nu \\
&= -\frac{m}{\sqrt{\int_0^1 du\dot{x}^2}}\ddot{x}_a + ieF_{a\nu}\dot{x}^\nu
\end{aligned} \tag{2.25}$$

Putting this equal to zero gives EOM.

So final expression for one loop effective action would be of the form

$$W^{\mathbb{E}}(A) = -\left(\frac{2\pi}{ma}\right)^{1/2}\det\left[\left(\frac{\delta^2 S_{eff}}{\delta x_\nu(u')\delta x_\mu(u)}\right)\Big|_{\bar{x}}\right]^{-1/2}\exp[-S_{\text{eff}}(\bar{x})] \tag{2.26}$$

but as is well-known in an Instanton calculation, integration over zero modes will be replaced by integration over collective co-ordinated thus giving some extra factor as we'll show in section 2.1.3. In the above equation $\bar{x}$ is solution to Euler-Lagrange equation with action S_{eff}. The det factor will be evaluated separately in the section2.1.3.

2.1.2 Instanton Solution

- Electric Field :-

  Consider a EM background corresponding to the time-dependent Electric field pointing in x_3 direction. In Euclidean space choosing a gauge in which non-zero component is only A_3 which is function of x_4. Implying

$$F_{\mu 1} = F_{\mu 2} = 0 \qquad F_{34} = -F_{43} = iE \tag{2.27}$$

  hence EOM for component 1 and 2 then gives

$$\ddot{x}_1 = \ddot{x}_2 = 0 \tag{2.28}$$

which from the periodic constraints $x_\mu(0) = x_\mu(1)$ implies

$$\dot{x}_1 = \dot{x}_2 = 0 \tag{2.29}$$

hence from condition $\dot{x}^2 = a^2$ we get $\dot{x}_3^2 + \dot{x}_4^2 = a^2$.

On the other hand for components 3 and 4, we get

$$m\ddot{x}_3 = ieaF_{34}\dot{x}_4 \qquad m\ddot{x}_4 = ieaF_{43}\dot{x}_3 \tag{2.30}$$

After Integrating first equation w.r.t u we get $m\dot{x}_3 = -ieaA_3$ putting this in $\dot{x}_3^2 + \dot{x}_4^2 = a^2$ gives

$$\dot{x}_4 = \sqrt{\left(a^2 + \left(\frac{eaA_3}{m}\right)^2\right)} \tag{2.31}$$

So given A_3 one can find x_4 and also x_3.

Action S_{eff} can be simplified further to give

$$S_{\text{eff}} = ma + ie\int_0^1 du\ A_3(x_4).\dot{x}_3 = \frac{m}{a}\int_0^1 du\dot{x}_4^2 \tag{2.32}$$

For the case of constant electric field (E) background we take gauge $A_3 = -iEx_4$ corresponding to the Electric field in x_3 direction. After substituting this gauge choice in eq.(2.31) gives x_4 and using $\dot{x}_3^2 + \dot{x}_4^2 = a^2$ we can find x_3.

$$x_3 = \frac{m}{eE}\cos\left(\frac{eEau}{m}\right) \qquad x_4 = \frac{m}{eE}\sin\left(\frac{eEau}{m}\right) \tag{2.33}$$

by imposing periodic boundary condition $x_3(u) = x_3(u+1)$ we find

$$a = 2\pi pR = \frac{m2p\pi}{eE}$$

Thus the trajectory for particles is given by[62][16]

$$x_3 = R\cos(2p\pi u) \qquad x_4 = R\sin(2p\pi u) \tag{2.34}$$

This represents circle in $x_3 - x_4$ plane with radius $R = m/eE$. Action $S_{\text{eff}}(\bar{x})$ can easily be calculated from eq.(2.32):

$$S_{\text{eff}}(\bar{x}) = \frac{m^2p\pi}{eE} \tag{2.35}$$

- Electric field parallel to Magnetic field :-

  For the case of $E \parallel B$ where E and B are in x_3 direction[1] , the components of Field tensor will be

$$F_{12} = -F_{21} = B; \quad F_{34} = -F_{43} = iE \tag{2.36}$$

  Substituting this in eq.(2.24) we get

$$\begin{aligned} m\ddot{x}_1 &= iea B\dot{x}_2 \qquad m\ddot{x}_2 = -iea B\dot{x}_1 \\ m\ddot{x}_3 &= -eaE\dot{x}_4 \qquad m\ddot{x}_4 = eaE\dot{x}_3 \end{aligned} \tag{2.37}$$

  We note from above that the equations for x_1, x_2 and x_3, x_4 are decoupled and the set of equations for x_3, x_4 are same as that for constant electric field case eq.(2.30). The set of equations for x_1, x_2 case give rise to hyperbolic solution which fails to satisfy periodic boundary conditions $x_\mu(0) = x_\mu(1)$ hence the only solution for x_1 and x_2 is trivial solution. This suggest that the $\bar{x}(u)$ is same as that for the case of constant electric field eq.(2.34). Hence S_{eff} remains same as given by eq.(2.35).

2.1.3 One-loop Pre-factor

- Electric case:-

  We define operator $M_{\mu\nu}$ as [62][27]

$$M_{\mu\nu} := \frac{\delta^2 S_{\text{eff}}}{\delta x_\nu(u')\delta x_\mu(u)} = -\left[\frac{m\delta_{\mu\nu}}{\sqrt{\int \dot{x}^2\, du}}\frac{d^2}{du^2} - ieF_{\mu\nu}\frac{d}{du}\right]\delta(u-u') - \frac{m\ddot{x}_\mu(u)\ddot{x}_\nu(u')}{[\int \dot{x}^2\, du]^{3/2}} \tag{2.38}$$

[1] A very important point to note is that the quantity of interest- the vacuum decay rate per unit space-time volume (Γ) is relativistically invariant while on the other hand as we'll see in section2.3 our final expression will not. The reason for this is because we have already chosen a frame in which E and B are parallel-which is so called the center of field frame[63]. For a general $\vec{E}$ and $\vec{B}$ one can always go to a such that frame $\vec{E}$ and $\vec{B}$ in that frame is parallel. Given a general $\vec{E}$ and $\vec{B}$ such frame moves with velocity vector

$$\frac{\vec{V}}{1+|V|^2} = \frac{\vec{E}\times\vec{B}}{|E|^2+|B|^2}$$

The E and B in this new frame can now be found by Lorentz transforming to the given frame.

Derivation is as presented below:

$$\int d^4q \, \frac{\delta^2 S_{\text{eff}} \eta(q)}{\delta x_a(p) \delta x_b(q)} = \int d^4q \, \frac{\delta^2 \left[m\sqrt{\int_0^1 \dot{x}^2 du} + ie\int_0^1 A.\dot{x}du \right] \eta(q)}{\delta x_a(p) \delta x_b(q)}$$
$$= \int d^4q \, \frac{\delta}{\delta x_a(p)} \left[\frac{-m\ddot{x}_b(q)}{\sqrt{\int_0^1 \dot{x}^2 du}} + iF_{b\mu}\dot{x}^\mu(q) \right] \eta(q)$$
$$= \int d^4q \, \frac{-m}{\sqrt{\int_0^1 \dot{x}^2 du}} \frac{d^2}{dq^2} (\delta(q-p)\delta_b^a) \eta(q) - \int d^4q \, \frac{m\ddot{x}_a(p)\ddot{x}_b(q)}{\left(\sqrt{\int_0^1 \dot{x}^2 du}\right)^3} \eta(q)$$
$$+ \int d^4q \, \left[i\partial_a F_{b\mu}\dot{x}^\mu \delta(q-p) + iF_{ba} \frac{d}{dq} \delta(p-q) \right] \eta(q) \tag{2.39}$$

For the case of constant fields this, after relabeling indices, we get $M_{\mu\nu}$ as given in eq.(2.38). For the case of electric field only, substituting Instanton solution eq.(2.34), we get:

$$M_{\mu\nu} = \left[-\frac{eE}{2p\pi} \frac{d^2}{du^2} \delta_{\mu\nu} + ieF_{\mu\nu} \frac{d}{du} \right] \delta(u-u') - \frac{2p\pi eE}{R^2} \bar{x}_\mu(u) \bar{x}_\nu(u') \tag{2.40}$$

Where we denoted $\bar{x}$ to be the solution found in eq.(2.34). We want to calculate $\det'[M]$ where ' overhead represents barring zero modes. We use matrix determinant lemma which states:

$$\det(A + PQ^T) = \det(\mathrm{A}) \left(1 + Q^T A^{-1} P\right) \tag{2.41}$$

Hence determinant eq.(2.40) reduces to[27]

$$\det'[M] = \det'[L] \left[1 - 2p\pi \frac{eE}{R^2} \int \int du\,du' \bar{x}_\mu(u) (L^{-1})_{\mu\nu} \bar{x}_\nu(u') \right] (-2p\pi eE) \tag{2.42}$$

The last factor of $-2p\pi eE$ has been factored out since it is the only negative eigenvalue of matrix M with eigenvector $\bar{x}_\mu(u')/R$ corresponding to changing the loop radius.

There are in total five zero modes for $L_{\mu\nu}$: Four of which corresponds to translation of loop with Eigenvectors

$$[1,0,0,0],\ [0,1,0,0],\ [0,0,1,0],\ [0,0,0,1] \tag{2.43}$$

There is 1 zero mode corresponding to u-translation with Eigenvector of $\frac{1}{p}\frac{d\bar{x}^{\mu}}{du}$. These zero modes must be accounted for by replacing integration over dc_i to du and d^4x. While doing this Jacobian factors must be taken into account. For the case of proper time translation this gives a factor of $2\pi R/(2\pi)^{1/2}$, which is obtained by replacing integration over $dc_0/(2\pi)^{1/2}$ with $Jdu/(2\pi)^{1/2}$ the Jacobian J turns out to be $2\pi R$. For the case of loop translations the integration over $dc_1dc_2dc_3dc_4/(2\pi)^2$ with $V_4^{\mathbb{E}}$(Four Volume).

Next, we need to find the eigenvalues and eigenvectors corresponding to matrix L which are as given below [62]

$$L = \begin{bmatrix} -\frac{eE}{2p\pi}\frac{d^2}{du^2} & 0 & 0 & 0 \\ 0 & -\frac{eE}{2p\pi}\frac{d^2}{du^2} & 0 & 0 \\ 0 & 0 & -\frac{eE}{2p\pi}\frac{d^2}{du^2} & -eE\frac{d}{du} \\ 0 & 0 & eE\frac{d}{du} & -\frac{eE}{2p\pi}\frac{d^2}{du^2} \end{bmatrix} \tag{2.44}$$

The eigenvalues are $2\pi eE(n^2/p-n)$ with corresponding eigenvector of

$$(0,0,\cos(2n\pi u),\sin(2n\pi u)) \quad (0,0,\sin(2n\pi u),-\cos(2n\pi u)) \tag{2.45}$$

and $2\pi eE(n^2/p+n)$ with corresponding eigenvector of

$$(0,0,\sin(2n\pi u),\cos(2n\pi u)) \quad (0,0,\cos(2n\pi u),-\sin(2n\pi u)) \tag{2.46}$$

where n runs from 1 to ∞. There are eigenvalues and eigenvectors corresponding to trivial parts of matrix (1-2) which are given by

$$(\cos(2\pi nu),0,0,0),\ (\sin(2\pi nu),0,0,0),\ (0,\cos(2\pi nu),0,0),\ (0,\sin(2\pi nu),0,0) \tag{2.47}$$

with eigenvalue of $2\pi eEn^2/p$ where n runs from $1,2,\cdots,\infty$.

Since we want to calculate $\det'[L]$ which is given by

$$\det'[L] = N\prod_{n\neq 0,p}(2\pi eE(n^2/p-n))^2\prod_{n\neq 0}(2\pi eEn^2/p)^2 \tag{2.48}$$

where both eigenvalues are taken care of by taking product over $-\infty$ to ∞. The normalization factor N comes from converting Feynman path integral eq.(2.21) to determinant eq.(2.26) and can be fixed by using the following identity[27]

$$\int_{x(0)=x(1)} Dx\exp\Big[-\int\frac{m^2}{4T_0}\dot{x}^2\,du\Big] = N^{-1/2}\Big(\det'\Big[\Big(-\frac{m^2}{2T_0}\frac{d^2}{du^2}\Big)\Big]\Big)^{-1/2} = \Big(\frac{m^2}{4\pi T_0}\Big)^2 \tag{2.49}$$

obtained by comparing it with the free particle propagator

$$\int Dx(t)\exp\Big[\frac{i}{\hbar}\int\frac{m}{2}\dot{x}^2\,dt\Big] = \Big(\frac{m}{2\pi i\hbar(t_f-t_i)}\Big)^{1/2}\exp\Big[\frac{im(x_f-x_i)^2}{2\hbar(t_f-t_i)}\Big] \tag{2.50}$$

Using eq.(2.49) we get

$$\det'[L] = \left(\frac{(4\pi T_0)^2}{m^4}\right)^2 \frac{\prod_{n\neq 0,p}\big(2\pi eE(n^2/p-n)\big)^2\prod_{n\neq 0}(2\pi eEn^2/p)^2}{\det'[-\frac{m^2d^2}{2T_0du^2}]} \tag{2.51}$$

denominator in the last term is just like the trivial part of matrix L, hence we get

$$\det'[L] = \Big(\frac{(4\pi T_0)^2}{m^4}\Big)^2\frac{1}{(2p\pi eE)^2}\prod_{n\neq 0,p}\frac{\big((n^2/p-n)\big)^2}{n^4/p^2} \tag{2.52}$$

The infinite product can be written as

$$\prod_{n\neq 0,n\neq p}\frac{\big((n^2/p-n)\big)^2}{n^4/p^2} = \prod_{n\neq 0,n\neq p}(1-\frac{p}{n})^2 \tag{2.53}$$

We use following identity [64] to get infinite product

$$\frac{\sin[\pi pz]}{p\pi z} = \prod_{n=1}^{\infty}\Big(1-\frac{z^2p^2}{n^2}\Big) \tag{2.54}$$

which could be rewritten in the following way

$$\frac{\sin[\pi pz]}{p\pi z} = \prod_{n=1}^{\infty}\left(1-\frac{z^2p^2}{n^2}\right)$$
$$= \prod_{n=1}^{\infty}\left(1-\frac{zp}{n}\right)\left(1+\frac{zp}{n}\right)$$
$$= \prod_{n=1}^{\infty}\left(1-\frac{zp}{n}\right)\prod_{n=-1}^{-\infty}\left(1-\frac{zp}{n}\right) \tag{2.55}$$
$$= \prod_{n=-\infty}^{\infty}\left(1-\frac{zp}{n}\right)$$
$$= (1-z)\prod_{n\neq p}\left(1-\frac{zp}{n}\right)$$

Then we can reduce

$$\lim_{z\to 1}\frac{\sin[\pi pz]}{(1-z)p\pi z} = \lim_{z\to 1}\prod_{n\neq p}\left(1-\frac{zp}{n}\right)$$
$$(-1)^{p+1} = \prod_{n\neq p}\left(1-\frac{p}{n}\right) \tag{2.56}$$

Using this and $T_0 = m^2 p\pi/eE$ we get

$$\det{}'[L] = \left(\frac{8p\pi^3(-1)^{p+1}}{e^3E^3}\right)^2 \tag{2.57}$$

The only part remaining to calculate is the non-local part:

$$\left[1-2p\pi\frac{eE}{R^2}\int\int du\,du'\bar{x}_\mu(u)\,(L'^{-1})_{\mu\nu}\,\bar{x}_\nu(u')\right] \tag{2.58}$$

which as we'll show comes out be 1[27]. Where L' is only the non-trivial part of matrix $(3-4)$. The Green's function $\left(L'^{-1}\right)_{\mu\nu}$ can be obtained from the spectral representation according to which $L'^{-1} = Q\Lambda^{-1}Q^{-1}$ where Q is the matrix with column as eigenvectors of L' and Λ is the diagonal matrix with eigenvalues as diagonal entries

$$\left(L'^{-1}\right) = \sum_{\substack{n\neq 0\\ n\neq p\\ n=-\infty}}^{\infty}\frac{1}{2\pi eE(n^2/p-n)}\begin{pmatrix}\cos(2\pi n(u-u')) & -\sin(2\pi n(u-u'))\\ \sin(2\pi n(u-u')) & \cos(2\pi n(u-u'))\end{pmatrix} \tag{2.59}$$

It can be checked easily that L' acting on L'^{-1} indeed gives $\mathbb{I}_{2\times 2}\delta(u-u')$. As, when L' acts on L'^{-1} the eigenvalue $2\pi eE(n^2/p-n)$ pops out canceling the same factor in the denominator. The sum over n from $-\infty$ to ∞ gives zero in the off-diagonal parts and the identity times delta function in the diagonal part. And thus using x_3 and x_4 as found in (2.34) we get

$$\int_0^1 du \int_0^1 du' \, \bar{x}_\mu(u) \left(L'^{-1}\right)_{\mu\nu} \bar{x}_\nu(u') = 0. \tag{2.60}$$

Taking into account all the pieces (contribution from zero eigenvalues, $\det'(L)$, negative eigenvalue, factor of $\pm$ i/2 [65], $-(2\pi/ma)^{1/2}$ in eq.(2.26)) into account we get

$$\begin{aligned} \mathscr{P}^{\mathbb{E}}_{0,sc} &= V_4^{\mathbb{E}} \cdot (2\pi)^{1/2} \frac{m}{eE} \cdot - \left(\frac{2\pi}{ma}\right)^{1/2} \cdot \frac{-i}{2} \cdot \frac{1}{(2\pi peE)^{1/2}} \cdot \frac{e^3E^3(-1)^{p+1}}{8\pi^3 p} \\ &= \frac{V_4^{\mathbb{E}} e^2E^2 i(-1)^{p+1}}{16\pi^3 p^2} \end{aligned} \tag{2.61}$$

Where $\mathscr{P}^{\mathbb{E}}_{0,sc}$ is the pre-exponential factor for vacuum decay rate of Scalars at zero temperature in constant E background. Then the expression for $W^{\mathbb{E}}[A]$ is given by

$$W^{\mathbb{E}}[A] = \sum_{p=1}^{\infty} \frac{iV_4^{\mathbb{E}}(-1)^{p+1}e^2E^2}{16\pi^3 p^2} \exp\left[-\frac{m^2 p\pi}{eE}\right] \tag{2.62}$$

Hence for scalar case decay rate per unit space-time volume, given by eq.(2.6), is [66]

$$\Gamma^{\mathbb{E}}_{0,sc} = \sum_{p=1}^{\infty} \frac{(-1)^{p+1}e^2E^2}{8\pi^3 p^2} \exp\left[-\frac{m^2 p\pi}{eE}\right] \tag{2.63}$$

- Electric field parallel to Magnetic field

The only change from electric field case is that L picks up some off diagonal term in $\mu,\nu \in 1,2$ because those components from $F_{\mu\nu}$ are non-zero. It is easy to see that, which is also evident from eom, that the $1,2$ part of matrix L is decoupled from $3,4$ part. So the eigenvalues and eigenvectors for $3,4$ part which we found in the electric case remains same, the only change will be the new eigenvalues and eigenvectors for $1,2$ part.

$$L = \begin{bmatrix} -\frac{eE}{2p\pi}\frac{d^2}{du^2} & ieB\frac{d}{du} & 0 & 0 \\ -ieB\frac{d}{du} & -\frac{eE}{2p\pi}\frac{d^2}{du^2} & 0 & 0 \\ 0 & 0 & -\frac{eE}{2p\pi}\frac{d^2}{du^2} & -eE\frac{d}{du} \\ 0 & 0 & eE\frac{d}{du} & -\frac{eE}{2p\pi}\frac{d^2}{du^2} \end{bmatrix} \tag{2.64}$$

The additional eigenvalues are $2\pi eE\big(-\frac{iBn}{E}+\frac{n^2}{p}\big)$ with corresponding eigenvector of

$$(1,i,0,0)\exp[2\pi inu],\ (i,-1,0,0)\exp[2\pi inu] \tag{2.65}$$

and $2\pi eE\big(\frac{iBn}{E}+\frac{n^2}{p}\big)$ with corresponding eigenvector of

$$(1,-i,0,0)\exp[2\pi inu],\ (i,1,0,0)\exp[2\pi inu] \tag{2.66}$$

In both the cases $n \in 1,2,\cdots,\infty$.

Following the same procedure as in the previous section

$$\det{}'[L] = N\prod_{n\neq 0,p}(2\pi eE(n^2/p^2-n))^2\prod_{n\neq 0}\big(2\pi eE(n^2/p^2-\frac{iBn}{E})\big)^2 \tag{2.67}$$

while taking care of N as in the constant E case, we get

$$\det{}'[L] = \Big(\frac{(4\pi T_0)^2}{m^4}\Big)^2\frac{1}{(2p\pi eE)^2}\prod_{n\neq 0,p}\frac{\big((n^2/p-n)\big)^2}{n^4/p^2}\prod_{n\neq 0,n=-\infty}^{\infty}\frac{\Big[2\pi eE(\frac{n^2}{p}-\frac{iBn}{E})\Big]^2}{(2\pi eE)^2n^4/p^2} \tag{2.68}$$

first three terms in the above expression are calculated in the constant E case eq.(2.57), the last term containing infinite product can be evaluated as follows

$$\begin{aligned}\prod_{n\neq 0,n=-\infty}^{\infty}\frac{\Big[2\pi eE(\frac{n^2}{p}-\frac{iBn}{E})\Big]^2}{(2\pi eE)^2n^4/p^2} &= \prod_{n\neq 0,n=-\infty}^{\infty}\big(1-\frac{iBp}{En}\big)^2 \\ &= \prod_{n=1}^{\infty}\big(1-\frac{iBp}{En}\big)^2\big(1+\frac{iBp}{En}\big)^2 \\ &= \prod_{n=1}^{\infty}\big(1+\frac{B^2p^2}{E^2n^2}\big)^2 \\ &= \Big(\frac{E\sinh(p\pi B/E)}{p\pi B}\Big)^2\end{aligned} \tag{2.69}$$

since [64]

$$\frac{\sinh(k\pi)}{k\pi} = \prod_{n=1}^{\infty}(1+\frac{k^2}{n^2}) \tag{2.70}$$

then using eq.(2.57) and eq.(2.69) we get

$$\det{}'[L] = \Big(\frac{8p\pi^3(-1)^{p+1}}{e^3E^3}\Big)^2\Big(\frac{E\sinh(p\pi B/E)}{p\pi B}\Big)^2 \tag{2.71}$$

The non-local part in eq.(2.42) is still 1, since as we saw x_1 and x_2 are trivial hence making the the corresponding part of product in the non-local part vanish. And as though x_3 and x_4 factors are non-trivial, they are already shown to give trivial result in just Electric field case. The decoupling between $1,2$ and $3,4$ components play crucial role while doing this.

So the final expression of Pre-exponential factors after taking into account ($\det'[L]$, negative eigenvalue, contribution from zero eigenvalues, factor of $\pm$ i/2, factor of $-(2\pi/ma)^{1/2}$ from eq.(2.26)):

$$\begin{aligned}\mathscr{P}^{\text{EB}}_{0,sc} &= V_4^{\mathbb{E}}\cdot(2\pi)^{1/2}\frac{m}{eE}\cdot -\Big(\frac{2\pi}{ma}\Big)^{1/2}\cdot\frac{-i}{2}\cdot\frac{1}{(2\pi peE)^{1/2}}\cdot\frac{e^3E^3(-1)^{p+1}}{8\pi^3 p}\cdot\frac{p\pi B}{E\sinh(p\pi B/E)}\\ &= \frac{V_4^{\mathbb{E}}(-1)^{p+1}e^2E^2 i}{16\pi^3p^2}\frac{p\pi B}{E\sinh(p\pi B/E)}\end{aligned} \tag{2.72}$$

Where $\mathscr{P}^{\text{EB}}_{0,sc}$ is the pre-exponential factor for vacuum decay rate of Scalars at zero temperature in constant E background. Then the expression for $W^{\mathbb{E}}[A]$ is given by

$$W^{\mathbb{E}}[A] = \sum_{p=1}^{\infty}\frac{iV_4(-1)^{p+1}e^2EB}{16\pi^2p\sinh(p\pi B/E)}\exp\left[-\frac{m^2p\pi}{eE}\right] \tag{2.73}$$

Hence decay rate per unit space-time volume for scalar in $E \parallel B$ case, according to eq.(2.6), is [17]

$$\Gamma^{\text{EB}}_{0,sc} = \sum_{p=1}^{\infty}\frac{(-1)^{p+1}e^2EB}{8\pi^2p\sinh(p\pi B/E)}\exp\Big[-\frac{m^2p\pi}{eE}\Big] \tag{2.74}$$

which reduces to eq.(2.63) in the limit $B\rightarrow 0$.

2.2 Finite Temperature Case

2.2.1 Instanton solution and exponential factors $T \neq 0$

- Electric Field

  For calculating finite temperature vacuum decay rate for scalar particles in presence of constant electromagnetic field, we need to calculate Imaginary part of Euclidean scalar QED Effective action per unit four volume. Same as in the case of zero temperature one can write (2.21), but with an additional condition that $x_4(0) \equiv x_4(0) + n\beta$ for $n \in \mathbb{Z}$[67], where β^{-1} is identified with temperature. The one-loop euclidean effective action for finite temperature in the case of scalar QED is then given by

$$W^{\mathbb{E}}(A) = -\sum_{n\in\mathbb{Z}} \int_0^\infty \frac{dT}{T} \int dx \langle x | \exp(-T(-D^2)) | x + n\beta\hat{e}_4 \rangle e^{-m^2 T}$$
$$= \sum_{n\in\mathbb{Z}} -\sqrt{\frac{2\pi}{m}} \int_{\substack{x_4(0)\equiv x_4(0)+n\beta \\ x(0)=x(1)}} [dx_\mu] \frac{1}{[\int_0^1 \dot{x}^2 du]^{1/4}} \exp\left[-m\sqrt{\int_0^1 \dot{x}^2 du} - ie\int_0^1 A.\dot{x} du \right] \tag{2.75}$$

  We have taken weak field approximation to arrive at step 2 of above equation. Comparing above equation with eq.(2.21) we see that in addition to satisfy $x_\mu(0) = x_\mu(1)$ as in the case of zero temperature case, x_μ should satisfy an additional constraint of periodicity in x_4 direction. This comes from a standard argument in the Instanton calculation in the context of quantum tunneling, where β is the total time taken by a particle to come back to initial position in an inverted potential[68].

  Considering the exponent in the eq.(2.75) as $-S_{\text{eff}}$, then equation of motion will be similar to eq.(2.24). A point to note is that in eq.(2.75), the case of $n = 0$ has already been evaluated in the zero temperature case. Hence only remaining part is that of $n \neq 0$ which would contribute to finite temperature correction to the vacuum decay rate expression. For finding finite temperature Instanton solution, we need to find solution of equation of motion eq.(2.24) where solution is periodic in x_4 direction with period $n\beta$. That is we have to find sections of zero temperature Instanton which are separated in time direction by $n\beta$. But for solution to exist $2R > n\beta$, implying $n_{max} = \lfloor 2R/\beta \rfloor$ (where $\lfloor x \rfloor$ is integer less than or equal to x). Hence no one-

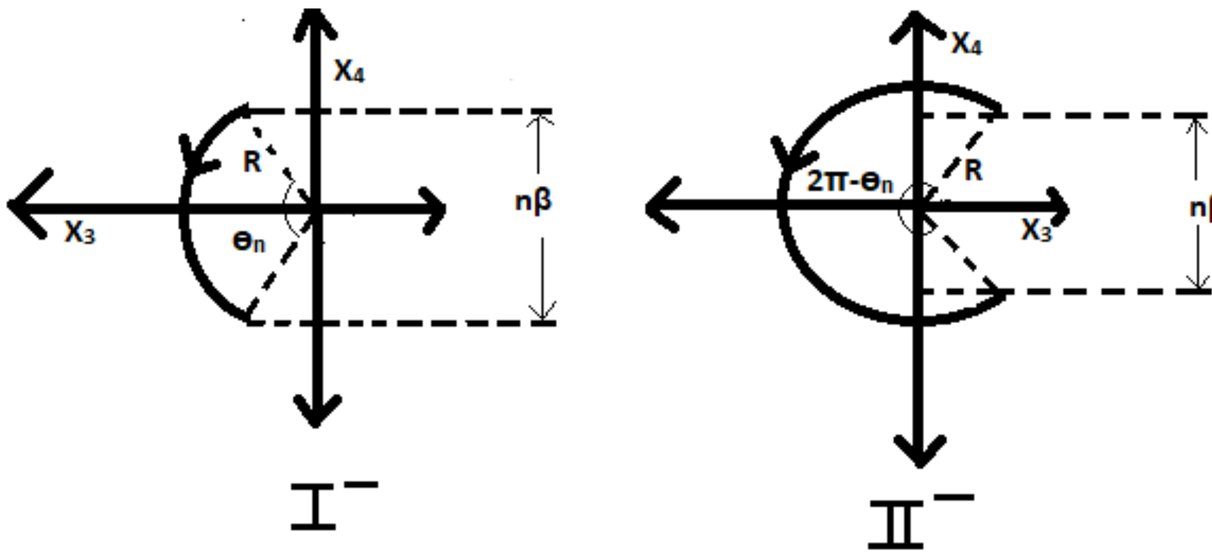

Figure 2.1: Finite temperature Instanton solutions satisfying periodic boundary condition (2.76) are shown. A sector of circle subtending angle θ_n (Fig. I^-) contribute to free energy, while the one with $2\pi - \theta_n$ (Fig. II^-) to the Schwinger pair production. In both figures $n\beta$ is separation along x_4 between endpoints of the path. R is the radius of circle which forms the solution at zero temperature.

loop thermal effects for $T < eE/2m (\equiv T_c)$.[27]

1. For $n \in \mathbb{Z}^-$ i.e. solution satisfying periodic boundary condition

$$x_4(1) = x_4(0) + n\beta; \qquad n \in \mathbb{Z}^- \tag{2.76}$$

There are two solutions satisfying the boundary condition as shown in Fig.2.1. For the smaller path (path I^-), subtending angle θ_n at the center, $\vartheta' = 2\pi p + \theta_n$ is the total angle subtended where p are the number of windings. The explicit solution ($\bar{x}^{\mathrm{T},I^-}$) is given by

$$x_3 = R\cos(\vartheta' u + \pi - \theta_n/2) \quad x_4 = R\sin(\vartheta' u + \pi - \theta_n/2) \tag{2.77}$$

we substitute this solution in $S_{\text{eff}}(x)$,

$$S_{\text{eff}}(x) = m\sqrt{\int_0^1 \dot{x}^2 du} + ie\int_0^1 du\, A_\mu(x).\dot{x}_\mu \tag{2.78}$$

For the gauge $A_3 = -iEx_4$, which corresponds to configuration where constant E

is in x_3 direction, we get

$$
\begin{aligned}
S_{\text{eff}}(\bar{x}^{\mathrm{T},I^-}) &= mR\vartheta' - mR\frac{\vartheta'}{2} + \frac{m^2}{2eE}\sin(\theta_n) \\
&= \frac{m^2}{2eE}\Big[2\pi p + 2\arcsin\big(\frac{nT_c}{T}\big)\Big] + \frac{nm}{2T}\sqrt{1-\frac{n^2T_c^2}{T^2}}
\end{aligned}
\tag{2.79}
$$

where $T_c = eE/2m$. From eq.(2.77) and eq.(2.76), we get relation between θ_n and Temperature (T) as follows

$$
\sin\Big(\frac{\theta_n}{2}\Big) = -\frac{n\beta}{2R} = -\frac{nT_c}{T}; \qquad n \in \mathbb{Z}^- \tag{2.80}
$$

For the longer path (path II^-), subtending angle $2\pi - \theta_n$ at the center, $\vartheta = 2\pi(p+1) - \theta_n$ is the total angle subtended where p are the number of windings. This solution will contribute to the pair production rate. Equation for the this solution ($\bar{x}^{\mathrm{T},II^-}$) is given by:

$$
x_3(u) = R\cos(\vartheta u + \theta_n/2) \quad x_4(u) = R\sin(\vartheta u + \theta_n/2) \tag{2.81}
$$

we substitute this solution in $S_{\text{eff}}(x)$, for gauge $A_3 = -iEx_4$, which corresponds to configuration where constant E is in x_3 direction, we get

$$
\begin{aligned}
S_{\text{eff}}(\bar{x}^{\mathrm{T},II^-}) &= mR\vartheta - mR\frac{\vartheta}{2} - \frac{m^2}{2eE}\sin(\theta_n) \\
&= \frac{m^2}{2eE}\Big[2\pi(p+1) - 2\arcsin\big(\frac{nT_c}{T}\big)\Big] - \frac{nm}{2T}\sqrt{1-\frac{n^2T_c^2}{T^2}}
\end{aligned}
\tag{2.82}
$$

where $T_c = eE/2m$ and R is the radius of circular Instanton. The relation between θ_n and n for this solution is same as eq.(2.80).

2. For $n \in \mathbb{Z}^+$ case i.e. solution satisfying periodic boundary condition

$$
x_4(1) = x_4(0) + n\beta; \qquad n \in \mathbb{Z}^+ \tag{2.83}
$$

There are two solutions satisfying the boundary condition as shown in Fig.2.2. For the smaller path (path I^+), subtending angle θ_n at the center, $\vartheta' = 2\pi p + \theta_n$ is the total angle subtended where p are the number of windings. The explicit solution $(\bar{x}^{\mathrm{T},I^+})$ is given by

$$x_3 = R\cos(\vartheta' u - \theta_n/2) \quad x_4 = R\sin(\vartheta' u - \theta_n/2) \tag{2.84}$$

we substitute this solution in $S_{\text{eff}}(x)$,

$$S_{\text{eff}}(x) = m\sqrt{\int_0^1 \dot{x}^2 du} + ie\int_0^1 du\, A_\mu(x).\dot{x}_\mu \tag{2.85}$$

For the gauge $A_3 = -iEx_4$, which corresponds to configuration where constant E is in x_3 direction, we get

$$\begin{aligned} S_{\text{eff}}(\bar{x}^{\mathrm{T},I^+}) &= mR\vartheta' - mR\frac{\vartheta'}{2} + \frac{m^2}{2eE}\sin(\theta_n) \\ &= \frac{m^2}{2eE}\Big[2\pi p + 2\arcsin\big(\frac{nT_c}{T}\big)\Big] + \frac{nm}{2T}\sqrt{1-\frac{n^2T_c^2}{T^2}} \end{aligned} \tag{2.86}$$

where $T_c = eE/2m$. From eq,(2.83) and eq.(2.84) we get relation between θ_n and n as follows

$$\sin\Big(\frac{\theta_n}{2}\Big) = \frac{n\beta}{2R} = \frac{nT_c}{T}; \qquad n \in \mathbb{Z}^+ \tag{2.87}$$

For the longer path (path II^+), subtending angle $2\pi - \theta_n$ at the center, $\vartheta = 2\pi(p+1) - \theta_n$ is the total angle subtended where p are the number of windings. This solution will contribute to the pair production rate. Equation for the this solution $(\bar{x}^{\mathrm{T},II^+})$ is given by:

$$x_3(u) = R\cos(\vartheta u + \pi + \theta_n/2) \quad x_4(u) = R\sin(\vartheta u + \pi + \theta_n/2) \tag{2.88}$$

we substitute this solution in $S_{\text{eff}}(x)$, for gauge $A_3 = -iEx_4$, which corresponds to configuration where constant E is in x_3 direction, we get

$$\begin{aligned} S_{\text{eff}}(\bar{x}^{\mathrm{T},II^+}) &= mR\vartheta - mR\frac{\vartheta}{2} - \frac{m^2}{2eE}\sin(\theta_n) \\ &= \frac{m^2}{2eE}\Big[2\pi(p+1) - 2\arcsin\big(\frac{nT_c}{T}\big)\Big] - \frac{nm}{2T}\sqrt{1-\frac{n^2T_c^2}{T^2}} \end{aligned} \tag{2.89}$$

where $T_c = eE/2m$ and R is the radius of circular Instanton. The relation between θ_n and n for this solution is same as eq.(2.87).

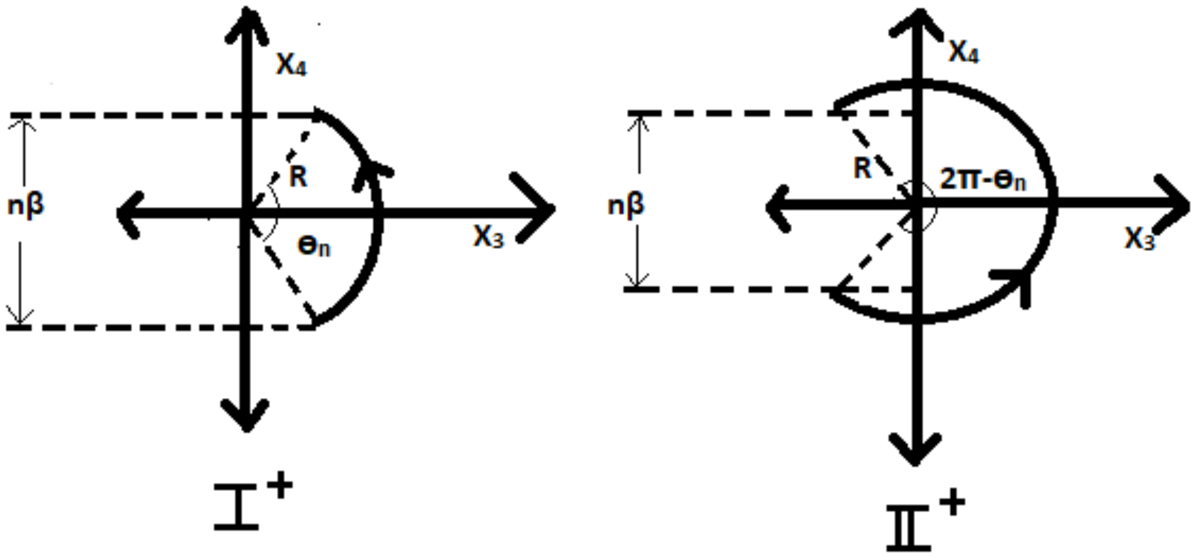

Figure 2.2: Finite temperature Instanton solutions satisfying periodic boundary condition eq.(2.83) are shown. A sector of circle subtending angle θ_n (Fig. I^+) contribute to free energy, while the one with $2\pi - \theta_n$ (Fig. II^+) to the Schwinger pair production. In both figures $n\beta$ is separation along x_4 between endpoints of the path. R is the radius of circle which forms the solution at zero temperature.

The solutions $\bar{x}^{\mathrm{T},II^-}$ and $\bar{x}^{\mathrm{T},II^+}$ contributing to the vacuum decay rate gave same expression for exponential factor. We will see in the later section that the contribution to pre-exponential factor of vacuum decay rate expression will also be same for both solutions. Hence, sum over $n \in \mathbb{Z}$ in eq.(2.75) will be replaced by twice sum over $n \in \mathbb{Z}^+$. Hence from now on we will consider solution $\bar{x}^{\mathrm{T},II^+}$ in the eq.(2.88) for the calculation purpose. Similarly, the solutions $\bar{x}^{\mathrm{T},I^-}$ and $\bar{x}^{\mathrm{T},I^+}$ contributing to the free energy of the created pair will contribute same. Hence from now on we will consider solution $\bar{x}^{\mathrm{T},I^+}$ in the eq.(2.84) for the calculation purpose.

- Electric Field parallel to Magnetic Field

Clearly for constant Electric field parallel to constant Magnetic field case the $S_{\text{eff}}(\bar{x}^{\mathrm{T},I^+})$ and $S_{\text{eff}}(\bar{x}^{\mathrm{T},II^+})$ remains same, as there are no non-trivial solution for x_1 and x_2 satisfying periodic boundary condition. Hence, exponential factor of correction to the scalar decay rate expression at finite temperature in the background of constant E and constant $E||B$ is $\exp(-S_{\text{eff}}(\bar{x}^{\mathrm{T},II^+}))$.

2.2.2 Pre-exponential factor at finite temperature

- Electric case:-

Similar to the case of zero-temperature, pre-exponential factor can be calculated using eq.(2.38). For finite temperature case, we substitute solution (2.88) in eq.(2.38)

$$M_{\mu\nu} := \frac{\delta^2 S}{\delta x_\nu(u')\delta x_\mu(u)}\Big|_{\bar{x}^{\mathrm{T},II^+}} = -\Big[\frac{eE\delta_{\mu\nu}}{\vartheta}\frac{d^2}{du^2} - ieF_{\mu\nu}\frac{d}{du}\Big]\delta(u-u') - \frac{\vartheta eE\bar{x}_\mu^{\mathrm{T},II^+}(u)\bar{x}_\nu^{\mathrm{T},II^+}(u')}{R^2} \tag{2.90}$$

using the matrix determinant lemma eq.2.41, we get

$$\det{}'[M] = \det{}'[L]\Big[1 - \vartheta\frac{eE}{R^2}\int\int du\,du'\,\bar{x}_\mu^{\mathrm{T},II^+}(u)\,(L^{-1})_{\mu\nu}\,\bar{x}_\nu^{\mathrm{T},II^+}(u')\Big] \tag{2.91}$$

where matrix L (using eq.(2.36)) is given by:

$$L = \begin{bmatrix} -\frac{eE}{\vartheta}\frac{d^2}{du^2} & 0 & 0 & 0 \\ 0 & -\frac{eE}{\vartheta}\frac{d^2}{du^2} & 0 & 0 \\ 0 & 0 & -\frac{eE}{\vartheta}\frac{d^2}{du^2} & -eE\frac{d}{du} \\ 0 & 0 & eE\frac{d}{du} & -\frac{eE}{\vartheta}\frac{d^2}{du^2} \end{bmatrix} \tag{2.92}$$

For calculating $\det'[L]$, we use trick given in [69], according to which

$$\left|\frac{\det'[L]}{\det'[\bar{L}]}\right| = \left|\frac{\prod\lambda_\alpha}{\prod\bar{\lambda}_\alpha}\right| = \left|\frac{\det\eta_\nu^\rho(1)}{\det\bar{\eta}_\nu^\rho(1)}\right| \tag{2.93}$$

where $\bar{L}$ is the matrix made out of L excluding all the non-diagonal terms. λ_α and $\bar{\lambda}_\alpha$ are the eigenvalues of L and $\bar{L}$ respectively. Since the eigen-spectrum for L is unknown; we use second equality in the above equation to calculate $\det'[L]$. The matrix $\eta_\nu^\rho(u)$ and $\bar{\eta}_\nu^\rho(u)$ satisfy following set of equations:

$$\begin{aligned} L_{\mu\nu}\eta_\nu^\rho(u) = 0;\ \eta_\nu^\rho(0) = 0;\ \dot{\eta}_\nu^\rho(0) = \delta_\nu^\rho \\ \bar{L}_{\mu\nu}\bar{\eta}_\nu^\rho(u) = 0;\ \bar{\eta}_\nu^\rho(0) = 0;\ \dot{\bar{\eta}}_\nu^\rho(0) = \delta_\nu^\rho \end{aligned} \tag{2.94}$$

For constant E case, the η matrix with appropriate boundary condition turns out to be

$$\eta = \begin{bmatrix} u & 0 & 0 & 0 \\ 0 & u & 0 & 0 \\ 0 & 0 & \frac{\sin\vartheta u}{\vartheta} & \frac{(-1+\cos\vartheta u)}{\vartheta} \\ 0 & 0 & \frac{(1-\cos\vartheta u)}{\vartheta} & \frac{\sin\vartheta u}{\vartheta} \end{bmatrix} \tag{2.95}$$

the $\det[\eta(1)] = 2(1-\cos\vartheta)/\vartheta^2$, which is always positive. The $\bar{\eta}$ matrix turns out to be $u\mathbb{I}_{4\times 4}$, hence the $\det[\bar{\eta}(1)] = 1$. We calculate $(N\det'[\bar{L}])^{-1/2}$ by substituting $T_0 = mR\vartheta/2$ in eq.(2.49). So we get,

$$\begin{aligned} (N\det'[L])^{-1/2} &= (N\det'[\bar{L}])^{-1/2}\sqrt{\frac{\vartheta^2}{2(1-\cos[\vartheta])}} \\ &= (-1)^p\left(\frac{eE}{2\pi\vartheta}\right)^2\sqrt{\frac{\vartheta^2}{2(1-\cos[\vartheta])}} \end{aligned} \tag{2.96}$$

factor of $(-1)^p$ is the Morse index corresponding to the solution eq.(2.88) as will be shown in appendix [27][32].

We still need to account for non-local part of eq.(2.91)

$$\left[1-\vartheta\frac{eE}{R^2}\int\int du\,du'\bar{x}_\mu^{\mathrm{T},II^+}(u)\,(L^{-1})_{\mu\nu}\,\bar{x}_\nu^{\mathrm{T},II^+}(u')\right] = \left[1-\vartheta\frac{eE}{R^2}\int\int du\,du'\bar{x}_\mu^{\mathrm{T},II^+}(u)\,G_{\mu\nu}\,\bar{x}_\nu^{\mathrm{T},II^+}(u')\right]$$

where $G_{\mu\nu}$ is green function satisfying following equation with Dirichlet boundary condition

$$L_{\mu\rho}G_{\rho\nu}(u-u') = \delta_{\mu\nu}\delta(u-u') \tag{2.97}$$

because of $L_{33} = L_{44}$ and $L_{43} = -L_{34}$, we'll get $G_{33} = G_{44}$ and $G_{43} = -G_{34}$. Exact expression for G_{33} and G_{43} as given in [27] is

$$\begin{aligned} G_{33} &= \frac{1}{2eE}\left[-\sin\left(\vartheta|u-u'|\right)+\sin\left(\vartheta u'\right)+\sin\left(\vartheta u\right)-\frac{4\sin\left(\frac{\vartheta}{2}u\right)\sin\left(\frac{\vartheta}{2}u'\right)\cos\left(\frac{\vartheta}{2}(u-u')\right)}{\tan\left(\frac{\vartheta}{2}\right)}\right] \\ G_{43} &= \frac{1}{2eE}\left[\mathrm{sgn}\left(u-u'\right)\left(\cos\left(\vartheta|u-u'|\right)-1\right)+\cos\left(\vartheta u'\right)-\cos\left(\vartheta u\right)\right] \\ &\quad -\frac{1}{2eE}\left[\frac{\sin\left(\vartheta\left(u-u'\right)\right)+\sin\left(\vartheta u'\right)-\sin\left(\vartheta u\right)}{\tan\left(\frac{\vartheta}{2}\right)}\right] \end{aligned} \tag{2.98}$$

the non-local part gives

$$\left[1-\frac{\vartheta eE}{R^2}\int\int du\,du'\bar{x}^{\mathrm{T},II^+}_{\mu}G_{\mu\nu}(u-u')\bar{x}^{\mathrm{T},II^+}_{\nu}(u')\right]=\frac{\vartheta}{2}\cot\left(\frac{\vartheta}{2}\right) \tag{2.99}$$

This quantity is negative for $0<\theta_n<\pi$ thus giving extra negative mode for longer paths (path II^+) hence contributing to decay rate. Substituting $\bar{x}^{\mathrm{T},II^-}$ in the place of $\bar{x}^{\mathrm{T},II^+}$ will give same answer thus contributing to decay rate expression. Substituting $\bar{x}^{\mathrm{T},I^+}$ in the place of $\bar{x}^{\mathrm{T},II^+}$ in above equation will replace ϑ' in the place of ϑ in the answer.

$$\left[1-\frac{\vartheta eE}{R^2}\int\int du\,du'\bar{x}^{\mathrm{T},I^+}_{\mu}G_{\mu\nu}(u-u')\bar{x}^{\mathrm{T},I^+}_{\nu}(u')\right]=\frac{\vartheta'}{2}\cot\left(\frac{\vartheta'}{2}\right) \tag{2.100}$$

This will be positive for $0<\theta_n<\pi$ thus contribute to free energy of produced pairs. The same holds true for solution $\bar{x}^{\mathrm{T},I^-}$ which will contribute to free energy of created pair.

Using eq.(2.91) we get

$$\begin{aligned}(\det{}'M)^{-1/2}&=(\det{}'L)^{-1/2}\left(\frac{2}{\vartheta\cot(\vartheta/2)}\right)^{1/2}\\&=(-1)^p\left(\frac{eE}{2\pi\vartheta}\right)^2\sqrt{\frac{\vartheta^2}{2(1-\cos[\vartheta])}}\left(\frac{2}{\vartheta\cot(\vartheta/2)}\right)^{1/2}\\&=(-1)^p\left(\frac{eE}{2\pi\vartheta}\right)^2\sqrt{\frac{\vartheta}{\sin(\vartheta)}}\end{aligned} \tag{2.101}$$

We take into account all the terms in the eq.(2.26) except the exponential factor. The pre-exponential factor is given by (Extra factor of $\pm i/2$ should also included as we are integrating over only one half of the Gaussian peak in the imaginary direction where the overall sign depends on the direction in which analytic continuation is performed[65]. Extra factor $\int d^4x=V_3\beta$ should also be included, owing to translational invariance.)

$$\begin{aligned}\mathscr{P}^{\mathrm{E}}_{\mathrm{T},sc}&=\frac{i}{2}\cdot V_3\beta\cdot(\det{}'M)^{-1/2}\cdot\left(\frac{2\pi}{ma}\right)^{1/2}\\&=\frac{i}{2}\cdot V_3\beta\cdot(-1)^p\left(\frac{eE}{2\pi\vartheta}\right)^2\sqrt{\frac{\vartheta}{\sin(\vartheta)}}\cdot\left(\frac{2\pi}{ma}\right)^{1/2}\end{aligned} \tag{2.102}$$

using eq.(2.87) we get

$$\sin(\vartheta) = \sin(-\theta_n) = -\frac{n\beta}{R}\sqrt{\left[1-\left(\frac{n\beta eE}{2m}\right)^2\right]} \tag{2.103}$$

we will remove the negative sign, since it has already been taken care by multiplication by $\pm i/2$ factor. Hence

$$\mathscr{P}^{\mathrm{E}}_{\mathrm{T},sc} = (-1)^p \frac{iV_3\beta}{2}\frac{(eE)^2}{(2\pi)^{3/2}(nm\beta)^{1/2}\vartheta^2}\left[1-\left(\frac{n\beta eE}{2m}\right)^2\right]^{-1/4} \tag{2.104}$$

- E parallel B:-

Similar to the case of zero-temperature, pre-exponential factor can be calculated using eq.(2.38). For finite temperature case, we substitute solution (2.81) in eq.(2.38)

$$M_{\mu\nu} := \frac{\delta^2 S}{\delta x_\nu(u')\delta x_\mu(u)}\Big|_{\bar{x}^{\mathrm{T},II^+}} = -\left[\frac{eE\delta_{\mu\nu}}{\vartheta}\frac{d^2}{du^2} - ieF_{\mu\nu}\frac{d}{du}\right]\delta(u-u') - \frac{\vartheta eE\bar{x}^{\mathrm{T},II^+}_\mu(u)\bar{x}^{\mathrm{T},II^+}_\nu(u')}{R^2} \tag{2.105}$$

using the matrix determinant lemma, we get

$$\det{}'[M] = \det{}'[L]\left[1-\vartheta\frac{eE}{R^2}\int\int du\,du'\bar{x}^{\mathrm{T},II^+}_\mu(u)\,(L^{-1})_{\mu\nu}\,\bar{x}^{\mathrm{T},II^+}_\nu(u')\right] \tag{2.106}$$

where matrix L (using eq.(2.36)) is given by:

$$L = \begin{bmatrix} -\frac{eE}{\vartheta}\frac{d^2}{du^2} & ieB\frac{d}{du} & 0 & 0 \\ -ieB\frac{d}{du} & -\frac{eE}{\vartheta}\frac{d^2}{du^2} & 0 & 0 \\ 0 & 0 & -\frac{eE}{\vartheta}\frac{d^2}{du^2} & -eE\frac{d}{du} \\ 0 & 0 & eE\frac{d}{du} & -\frac{eE}{\vartheta}\frac{d^2}{du^2} \end{bmatrix} \tag{2.107}$$

For calculating $\det'[L]$, we use trick given in [69], according to which

$$\left|\frac{\det'[L]}{\det'[\bar{L}]}\right| = \left|\frac{\prod\lambda_\alpha}{\prod\bar{\lambda}_\alpha}\right| = \left|\frac{\det\eta^\rho_\nu(1)}{\det\bar{\eta}^\rho_\nu(1)}\right| \tag{2.108}$$

where $\bar{L}$ is the matrix made out of L excluding all the non-diagonal terms. λ_α and $\bar{\lambda}_\alpha$ are the eigenvalues of L and $\bar{L}$ respectively. Since the eigen-spectrum for L is unknown we use second equality in the above equation to calculate $\det'[L]$. The matrix

$\eta^{\rho}_{\nu}(u)$ and $\bar{\eta}^{\rho}_{\nu}(u)$ satisfy following set of equations:

$$\begin{aligned} L_{\mu\nu}\eta^{\rho}_{\nu}(u) = 0;\ \eta^{\rho}_{\nu}(0) = 0;\ \dot{\eta}^{\rho}_{\nu}(0) = \delta^{\rho}_{\nu} \\ \bar{L}_{\mu\nu}\bar{\eta}^{\rho}_{\nu}(u) = 0;\ \bar{\eta}^{\rho}_{\nu}(0) = 0;\ \dot{\bar{\eta}}^{\rho}_{\nu}(0) = \delta^{\rho}_{\nu} \end{aligned} \tag{2.109}$$

For constant $E \parallel B$ case, the η matrix with appropriate boundary condition turns out to be

$$\eta = \begin{bmatrix} \frac{E}{\vartheta B}\sinh\left(\frac{B\vartheta u}{E}\right) & \frac{iE}{\vartheta B}\left(\cosh\left(\frac{B\vartheta u}{E}\right) - 1\right) & 0 & 0 \\ \frac{iE}{\vartheta B}\left(1 - \cosh\left(\frac{B\vartheta u}{E}\right)\right) & \frac{E}{\vartheta B}\sinh\left(\frac{B\vartheta u}{E}\right) & 0 & 0 \\ 0 & 0 & \frac{\sin\vartheta u}{\vartheta} & \frac{(-1+\cos\vartheta u)}{\vartheta} \\ 0 & 0 & \frac{(1-\cos\vartheta u)}{\vartheta} & \frac{\sin\vartheta u}{\vartheta} \end{bmatrix} \tag{2.110}$$

the $\det[\eta(1)] = \frac{4E^2}{\vartheta^4 B^2}(\cosh(B\vartheta/E) - 1)(1 - \cos\vartheta)$, which is always positive. The $\bar{\eta}$ matrix turns out to be $u\mathbb{I}_{4\times 4}$, hence the $\det[\bar{\eta}(1)] = 1$. We calculate $(N\det'[\bar{L}])^{-1/2}$ by substituting $T_0 = mR\vartheta/2$ in eq.(2.49). So we get,

$$\begin{aligned} (N\det'[L])^{-1/2} &= (N\det'[\bar{L}])^{-1/2}\sqrt{\frac{\vartheta^2}{2(1-\cos[\vartheta])}}\sqrt{\frac{\vartheta^2 B^2}{2E^2(\cosh(B\vartheta/E) - 1)}} \\ &= (-1)^p\left(\frac{eE}{2\pi\vartheta}\right)^2\sqrt{\frac{\vartheta^2}{2(1-\cos[\vartheta])}}\sqrt{\frac{\vartheta^2 B^2}{2E^2(\cosh(B\vartheta/E) - 1)}} \end{aligned} \tag{2.111}$$

factor of $(-1)^p$ is the Morse index corresponding to the solution eq.(2.88) which will be shown in the appendix.

We still need to account for non-local part of eq.(2.106)

$$\left[1 - \vartheta\frac{eE}{R^2}\int\int du\,du' x^{\mathrm{T},II^+}_{\mu}(u)\,(L^{-1})_{\mu\nu}\,x^{\mathrm{T},II^+}_{\nu}(u')\right] = \left[1 - \vartheta\frac{eE}{R^2}\int\int du\,du' \bar{x}^{\mathrm{T},II^+}_{\mu}(u)\,G_{\mu\nu}\,\bar{x}^{\mathrm{T},II^+}_{\nu}(u')\right] \tag{2.112}$$

Since x_1 and x_2 does not have a non-trivial solution satisfying the boundary condition, the combination containing $G_{11}, G_{12}, G_{21}, G_{22}$ are all trivial. The only remaining terms $G_{33}, G_{34}, G_{43}, G_{44}$ remains same as in the case of constant E eq.(2.98). Hence, the contribution for non-local part, in the constant $E \parallel B$ case, remains unaffected compared to constant E case. The contribution from non-local part is [27]

$$\frac{\vartheta}{2}\cot\left(\frac{\vartheta}{2}\right) \tag{2.113}$$

As mentioned in the earlier case. this quantity is manifestly negative thus giving extra negative mode for longer paths (path $II^{\pm}$) hence contributing to decay rate. Substituting ϑ' in the place of ϑ gives non-local part for shorter paths (path $I^{\pm}$) in fig.2.1, which will be always positive thus contribute to free energy of produced pairs. The only additional modification in comparison to constant electric field case is the last term in eq.(2.111). By taking that term into account, we get the pre-exponential factor for $E \parallel B$ case for finite temperature

$$\begin{aligned}\mathscr{P}^{\mathrm{EB}}_{\mathrm{T},sc} &= \mathscr{P}^{\mathrm{E}}_{\mathrm{T},sc} \cdot \sqrt{\frac{\vartheta^2 B^2}{2E^2(\cosh(B\vartheta/E)-1)}} \\ &= (-1)^p \frac{iV_3\beta}{2} \frac{(eE)^2}{(2\pi)^{3/2}(nm\beta)^{1/2}\vartheta^2}\left[1-\left(\frac{n\beta eE}{2m}\right)^2\right]^{-1/4} \cdot \sqrt{\frac{\vartheta^2 B^2}{2E^2(\cosh(B\vartheta/E)-1)}} \\ &= (-1)^p \frac{iV_3\beta}{4} \frac{e^2 EB}{(2\pi)^{3/2}(nm\beta)^{1/2}\vartheta \sinh\left(\frac{\vartheta B}{2E}\right)}\left[1-\left(\frac{n\beta eE}{2m}\right)^2\right]^{-1/4}\end{aligned} \tag{2.114}$$

2.3 Final Result

2.3.1 Zero Temperature

As already mentioned in section 1, the Schwinger pair production rate of scalar in constant electric background is (2.63) as already found in [66], and derived using Worldline Instanton method in [62]

$$\boxed{\Gamma^{\mathrm{E}}_{0,sc} = \sum_{p=1}^{\infty} \frac{(-1)^{p+1} e^2 E^2}{8\pi^3 p^2} \exp\left[-\frac{m^2 p\pi}{eE}\right]} \tag{2.115}$$

and for the background of constant electric field parallel to magnetic field is (2.74).

$$\boxed{\Gamma^{\mathrm{EB}}_{0,sc} = \sum_{p=1}^{\infty} \frac{(-1)^{p+1} e^2 EB}{8\pi^2 p \sinh(p\pi B/E)} \exp\left[-\frac{m^2 p\pi}{eE}\right]} \tag{2.116}$$

This result was derived in [17] which we derived here using worldline Instanton formalism[16]. This reduces to $\Gamma^{\mathrm{E}}_{0,sc}$ in the $B \to 0$ limit.

2.3.2 Finite Temperature

Schwinger pair production rate at finite temperature T in the background of constant electric field E is given by [27]

$$\Gamma^{\rm E}_{sc} = \Gamma^{\rm E}_{0,sc} + \Gamma^{\rm E}_{\rm T,sc} \tag{2.117}$$

where $\Gamma^{\rm E}_{\rm T,sc}$ (using eq.(2.89),(2.104) and (2.6))is given by:

$$\boxed{\begin{aligned}\Gamma^{\rm E}_{\rm T,sc} = \sum_{p=0}^{\infty}\sum_{n=1}^{n_{max}} 2(-1)^p \frac{(eE)^2}{(2\pi)^{3/2}(nm\beta)^{1/2}\vartheta^2}\left[1-\left(\frac{n\beta eE}{2m}\right)^2\right]^{-1/4} \\ \exp\left[-\frac{m^2}{2eE}\left[2\pi(p+1)-2\arcsin\left(\frac{nT_c}{T}\right)\right]+\frac{nm}{2T}\sqrt{1-\frac{n^2T_c^2}{T^2}}\right]\end{aligned}} \tag{2.118}$$

where $n_{max} = \lfloor 2R/\beta \rfloor$ and

$$\vartheta = 2\pi(p+1) - \theta_n = 2\pi(p+1) - 2\arcsin\left(\frac{nT_c}{T}\right) \tag{2.119}$$

This result was first derived by [27]. It is easy to note that $\Gamma^{\rm E}_{sc} = \Gamma^{\rm E}_{0,sc}$ for $T = 0$, since for $T < T_c$ there are no thermal corrections as Instanton solution does not exist.

Schwinger pair production rate at finite temperature T in the background of constant electric field E parallel to magnetic field B is

$$\Gamma^{\rm EB}_{sc} = \Gamma^{\rm EB}_{0,sc} + \Gamma^{\rm EB}_{\rm T,sc} \tag{2.120}$$

where $\Gamma^{\rm EB}_{\rm T,sc}$ (using (2.89),(2.114) and(2.6)) is given by:

$$\boxed{\begin{aligned}\Gamma^{\rm EB}_{\rm T,sc} = \sum_{p=0}^{\infty}\sum_{n=1}^{n_{max}} (-1)^p \frac{e^2EB}{(2\pi)^{3/2}(nm\beta)^{1/2}\vartheta\sinh\left(\frac{\vartheta B}{2E}\right)}\left[1-\left(\frac{n\beta eE}{2m}\right)^2\right]^{-1/4} \\ \exp\left[-\frac{m^2}{2eE}\left[2\pi(p+1)-2\arcsin\left(\frac{nT_c}{T}\right)\right]+\frac{nm}{2T}\sqrt{1-\frac{n^2T_c^2}{T^2}}\right]\end{aligned}} \tag{2.121}$$

where $n_{max} = \lfloor 2R/\beta \rfloor$ and

$$\vartheta = 2\pi(p+1) - \theta_n = 2\pi(p+1) - 2\arcsin\left(\frac{nT_c}{T}\right) \tag{2.122}$$

In the limit of $B \to 0$, Γ_{sc}^{EB} reduces to Γ_{sc}^{E}. Since in the $B \to 0$ limit

$$\sinh\left(\frac{\vartheta B}{2E}\right) \to \frac{\vartheta B}{2E} \tag{2.123}$$

thus $\Gamma_{\text{T},sc}^{\text{EB}} \to \Gamma_{\text{T},sc}^{\text{E}}$. This is the new result we derived using Worldline Instanton formalism. It is easy to note that $\Gamma_{sc}^{\text{EB}} = \Gamma_{0,sc}^{\text{EB}}$ for $T = 0$, since for $T < T_c$ there are no thermal corrections.

Chapter 3

Schwinger Pair Production in Spinor Electrodynamics

3.1 Zero Temperature Case

3.1.1 One Loop Effective Action

In Euclidean metric, the relation between $W^{\mathbb{E}}(A)$ and QED action S is given by

$$\exp(-W^{\mathbb{E}}(A)) = \int D\psi D\bar{\psi}\, exp[-S] \tag{3.1}$$

Where

$$S = \int d^4x\, \bar{\psi}(\not{D}+m)\psi + \frac{1}{4}F_{\mu\nu}^2 \tag{3.2}$$

with $\not{D} = \gamma_{\mathbb{E}}^{\mu} D_\mu = \gamma_{\mathbb{E}}^{\mu}(\partial_\mu + ieA_\mu)$, and $\bar{\psi} = \psi^\dagger \gamma_{\mathbb{E}}^4$. We have defined $A_\mu = (A_1, A_2, A_3, A_4)$ such that $A_4 = -iA_0$ and other components are same as Minkowaskian A_μ. The Electromagnetic field tensor is $F_{\mu\nu} = \partial_\mu A_\nu - \partial_\nu A_\mu$. The $\gamma_{\mathbb{E}}^{\mu}$ are Euclidean gamma matrices satisfying following algebra

$$\{\gamma_{\mathbb{E}}^{\mu}, \gamma_{\mathbb{E}}^{\nu}\} = 2\delta^{\mu\nu} \quad \gamma_{\mathbb{E}}^{5} = -\gamma_{\mathbb{E}}^{1}\gamma_{\mathbb{E}}^{2}\gamma_{\mathbb{E}}^{3}\gamma_{\mathbb{E}}^{4} \quad \{\gamma_{\mathbb{E}}^{5}, \gamma_{\mathbb{E}}^{\mu}\} = 0 \tag{3.3}$$

We choose following set of gamma matrices

$$\gamma^4_{\mathbb{E}} = \gamma^0_{\mathbb{M}} \quad \gamma^i_{\mathbb{E}} = -i\gamma^i_{\mathbb{M}} \tag{3.4}$$

where $\gamma^0_{\mathbb{M}}$ and $\gamma^i_{\mathbb{M}}$ are gamma matrices satisfying Clifford algebra. For the sake of simplicity we will drop subscript $\mathbb{E}$ from the Euclidean gamma matrices.

We use steepest decent approximation in RHS of eq.(3.1)

$$S[\psi,\bar{\psi}] = S[\psi_{cl},\bar{\psi}_{cl}] + \int \frac{\delta^2 S}{\delta\psi(y)\delta\bar{\psi}(x)}\bar{\eta}(x)\eta(y)d^4xd^4y \tag{3.5}$$

we have used multidimensional taylor expansion over Grassman variables η and $\bar{\eta}$. The $(\psi_{cl},\bar{\psi}_{cl})$ is a solution which make $\delta S/\delta\psi$ and $\delta S/\delta\bar{\psi}$ vanish. using eq.(3.1) and (3.5), we get

$$\begin{aligned}\exp(-W^{\mathbb{E}}(A)) &= \int D\psi D\bar{\psi}\, exp[-S] \\ &= \exp(-S(\psi_{cl}))\mathcal{N}(\det(\not{D}+m))\end{aligned} \tag{3.6}$$

As argued in scalar QED case, the factor of $\mathcal{N}$ and $\exp(-S(\psi_{cl}))$ can be dropped. We have used the formula path integral over Grassman variable

$$\prod_i \int d\theta_i^* d\theta_i e^{-\theta_i^* B\theta_i} = \det B \tag{3.7}$$

We can write

$$\det[\not{D}+m] = \det(\gamma_5)\det[\not{D}+m]\det(\gamma_5) = \det(-\not{D}+m) \tag{3.8}$$

thus we get,

$$\det(\not{D}+m) = \det{}^{1/2}(-\not{D}^2+m^2) = \det{}^{1/2}(-D^2+\frac{1}{2}e\sigma_{\mu\nu}F_{\mu\nu}+m^2) \tag{3.9}$$

where $D^2 = (\partial+ieA)^2$ and $\sigma_{\mu\nu} = -\frac{i}{2}[\gamma_\mu,\gamma_\nu]$ where γ_μ are Euclidean gamma matrices defined above.

Using above mathematical identities, we get

$$-W^{\mathbb{E}}(A) = \frac{1}{2}\mathrm{Tr}\ln[-D^2 + m^2 + \frac{1}{2}e\sigma_{\mu\nu}F_{\mu\nu}] \tag{3.10}$$

we use Frullani's integral

$$\mathrm{Tr}(\ln(P)) = -\int_0^\infty \frac{dT}{T}\,\mathrm{Tr}(\exp(-PT) - \exp(-T)) \tag{3.11}$$

to simplify further (dropping the second term as it will not contribute to imaginary part)

$$W^{\mathbb{E}}(A) = \frac{1}{2}\int_0^\infty \frac{dT}{T}\mathrm{Tr}\left[\exp\left[-T\left[-D^2 + \frac{1}{2}e\sigma_{\mu\nu}F_{\mu\nu} + m^2\right]\right]\right] \tag{3.12}$$

which could be written as

$$W^{\mathbb{E}}(A) = \frac{1}{2}\int_0^\infty \frac{dT}{T}\exp[-m^2T]\oint[dx_\mu]\exp\left[-\int_0^T d\tau\left[\frac{1}{4}\dot{x}^2 + ieA_\mu\dot{x}_\mu\right]\right]\,\mathrm{tr}\left[\exp\left[-\frac{1}{2}Te\sigma^{\mu\nu}F_{\mu\nu}\right]\right] \tag{3.13}$$

For the case of $E \parallel B$, the last term can be written as $4\cos[eET]\cosh[eBT]$ thus we get (after substituting $\tau = T\,u$, and $T \to T/m^2$)

$$W^{\mathbb{E}}(A) = 2\int_0^\infty \frac{dT}{T}\exp[-T]\oint[dx_\mu]\exp\left[-\left(\frac{m^2}{4T}\int_0^1 du\dot{x}^2 + ie\int_0^1 duA.\dot{x}\right)\right]\cos[eET/m^2]\cosh[eBT/m^2] \tag{3.14}$$

We perform T integral using saddle point approximation. Since the cos term in the exponential form gives imaginary part, hence it does not modify the saddle point[16]. Under the limit of $eB << m^2$ the cosh term does not modify the saddle point compared to scalar case. Hence the saddle point for the T integral turns out to be

$$T_0 = \frac{m}{2}\left(\int_0^1 \dot{x}^2\,du\right)^{1/2} \tag{3.15}$$

Hence, in the weak field limit-$eE << m^2$, the one-loop effective action for Spinor is given by

$$W^{\mathbb{E}}(A) = 2\sqrt{\frac{2\pi}{m}}\int[dx_\mu]\frac{1}{[\int_0^1 \dot{x}^2\,du]^{1/4}}\exp\left[-m\sqrt{\int_0^1 \dot{x}^2 du} - ie\int_0^1 A.\dot{x}du\right]\cos\left[\frac{eET_0}{m^2}\right]\cosh\left[\frac{eBT_0}{m^2}\right] \tag{3.16}$$

Considering terms in the exponential as $-S_{\text{eff}}(x)$ with Euler-Lagrange equation same as Scalar case eq.(2.24) (only in the weak field limit)

$$m\ddot{x}_\mu = ie\sqrt{\int_0^1 du\dot{x}^2}\, F_{\mu\nu}\dot{x}_\nu \tag{3.17}$$

So final expression for one-loop effective action for Spinor will look like

$$W^{\mathbb{E}}(A) = 2\left(\frac{2\pi}{ma}\right)^{1/2} \det\left[\left(\frac{\delta^2 S_{eff}}{\delta x_\nu(u')\delta x_\mu(u)}\right)\Big|_{\bar{x}}\right]^{-1/2} \exp[-S_{\text{eff}}(\bar{x})] \cos\left(\frac{eET_0}{m^2}\right) \cosh\left(\frac{eBT_0}{m^2}\right) \tag{3.18}$$

but as is well-known in an Instanton calculation, integration over zero modes will be replaced by integration over collective co-ordinates thus giving some extra factor as we've shown in section 2.1.3. Where $\bar{x}$ is solution to Euler-Lagrange equation with action S_{eff}. The det factor will be evaluated separately in the following sections.

3.1.2 Instanton Solution

- Electric Field :-

  The solution to eq.(3.17) are already found in the section2.1.2. The solution is given by

  $$x_3 = R\cos(2p\pi u) \qquad x_4 = R\sin(2p\pi u) \tag{3.19}$$

  This represents circle in $x_3 - x_4$ plane with radius $R = m/eE$. Action $S_{\text{eff}}(\bar{x})$ as already evaluated in eq.(2.35)

  $$S_{\text{eff}} = \frac{m^2 p\pi}{eE} \tag{3.20}$$

  Given the solution, we also get $a = 2p\pi R$ and $T_0 = ma/2 = m^2 p\pi/eE$. The extra factor in Spinor One-loop effective action which is

  $$\cos(eET_0/m^2)\cosh(eBT_0/m^2) \xrightarrow{B=0} (-1)^p \tag{3.21}$$

- Electric field parallel to Magnetic field :-

  For the case of $E \parallel B$ where E and B are in x_3 direction, the components of Field tensor will be $F_{12} = -F_{21} = B$ and $F_{34} = -F_{43} = iE$. As we argued in the case of scalar in section2.1.2, there are no non-trivial solution in $x_1 - x_2$ direction. This suggest that the $\bar{x}(u)$ is same as that for the case of constant electric field eq.(3.19). Hence S_{eff} remains same as given by eq.(3.20). The extra factor in Spinor One-loop effective action which is

$$\cos(eET_0/m^2)\cosh(eBT_0/m^2) \to (-1)^p \cosh(p\pi B/E) \tag{3.22}$$

since $T_0 = ma/2 = m^2 p\pi/eE$.

3.1.3 One-loop Pre-factor

- Electric case

  As we argued in section3.1.1, under the weak field approximation ($eE << m^2$, $eB << m^2$) the $S_{\text{eff}}(x)$ does not change as compared to scalar case. Hence, in this approximation the operator M in (2.38) also does not change nor does the $\det M$ as compared to the scalar case. Hence using eq.(2.61),

$$\begin{aligned} \mathscr{P}^{\mathbb{E}}_{0,sp} &= -2 \cdot \mathscr{P}^{\mathbb{E}}_{0,sc} \\ &= -2 \cdot \frac{V_4^{\mathbb{E}} e^2 E^2 i (-1)^{p+1}}{16\pi^3 p^2} \end{aligned} \tag{3.23}$$

  The only extra factor -2 need to be taken into account in the pre-exponential factor compared to scalar case (comparing eq.(3.18) and (2.26)).

  Then, one-loop effective action is given by

$$\begin{aligned} W_{\mathbb{E}} &= \sum_{p=1}^{\infty} \mathscr{P}^{\mathbb{E}}_{0,sp} \cdot (-1)^p \exp(-S_{\text{eff}}(\bar{x})) \\ &= 2 \sum_{p=1}^{\infty} \cdot \frac{V_4^{\mathbb{E}} e^2 E^2 i}{16\pi^3 p^2} \cdot \exp(-S_{\text{eff}}(\bar{x})) \\ &= \sum_{p=1}^{\infty} \frac{i V_4^{\mathbb{E}} e^2 E^2}{8\pi^3 p^2} \exp\left[-\frac{m^2 p\pi}{eE}\right] \end{aligned} \tag{3.24}$$

  Hence using eq.(2.6),

$$\Gamma^{\mathbb{E}}_{0,sp} = \sum_{p=1}^{\infty} \frac{e^2 E^2}{4\pi^3 p^2} \exp\left[-\frac{m^2 p\pi}{eE}\right] \tag{3.25}$$

- Electric field parallel to magnetic field case

As argued above the det$M$ does not change as compared to scalar case, hence using (2.72)

$$\begin{aligned}\mathscr{P}^{\text{EB}}_{0,sp} &= -2\cdot\mathscr{P}^{\text{EB}}_{0,sc}\\ &= -2\cdot\frac{V_4^{\mathbb{E}}(-1)^{p+1}e^2E^2 i}{16\pi^3 p^2}\frac{p\pi B}{E\sinh(p\pi B/E)}\end{aligned} \tag{3.26}$$

Then, one-loop effective action is given by

$$\begin{aligned}W_{\mathbb{E}} &= \sum_{p=1}^{\infty}\mathscr{P}^{\text{EB}}_{0,sp}\cdot(-1)^p\exp(-S_{\text{eff}}(\bar{x}))\cosh(p\pi B/E)\\ &= 2\sum_{p=1}^{\infty}\cdot\frac{V_4^{\mathbb{E}}(-1)^{2p}e^2E^2 i}{16\pi^3 p^2}\frac{p\pi B}{E\sinh(p\pi B/E)}\cdot\exp(-S_{\text{eff}}(\bar{x}))\cosh(p\pi B/E)\\ &= \sum_{p=1}^{\infty}\frac{iV_4^{\mathbb{E}}e^2EB}{8\pi^2 p}\exp\left[-\frac{m^2p\pi}{eE}\right]\coth[p\pi B/E]\end{aligned} \tag{3.27}$$

Hence using eq.(2.6), for the Spinor case in the background of constant electric field parallel to constant magnetic field the decay rate expression is given by [17]

$$\Gamma^{\text{EB}}_{0,sp} = \sum_{p=1}^{\infty}\frac{e^2EB\coth(p\pi B/E)}{4\pi^2 p}\exp\Big[-\frac{m^2p\pi}{eE}\Big] \tag{3.28}$$

which we re-derived here using Worldline Instanton method. This reduces to eq.(3.25) in the limit $B\to 0$.

3.2 Finite Temperature Case

3.2.1 Instanton solution and exponential factors $T \neq 0$

- Electric Field For calculating finite temperature vacuum decay rate for Spinor QED particles in presence of constant electromagnetic field, we need to calculate Imaginary part of Euclidean effective action of QED per unit four volume. Same as in the case of zero temperature one can write(3.18) , but with an additional condition that $x_4(0) \equiv x_4(0) + n\beta$[67]. The one-loop effective action for Spinor at finite temperature is given by

$$W^{\mathbb{E}}(A) = \sum_{n\in\mathbb{Z}} \frac{1}{2}\int_0^\infty \frac{dT}{T}\int dx \langle x|\exp(-T(-D^2+\frac{1}{2}e\sigma_{\mu\nu}F_{\mu\nu}))|x+n\beta\hat{e}_4\rangle e^{-m^2T}$$
$$= \sum_{n\in\mathbb{Z}} 2\sqrt{\frac{2\pi}{m}}\int_{\substack{x_4(0)\equiv x_4(0)+n\beta \\ x(0)=x(1)}} [dx_\mu]\frac{1}{[\int_0^1 \dot{x}^2\,du]^{1/4}}\exp\left[-m\sqrt{\int_0^1 \dot{x}^2 du} - ie\int_0^1 A.\dot{x}du\right]$$
$$\cos\left[\frac{eET_0}{m^2}\right]\cosh\left[\frac{eBT_0}{m^2}\right] \tag{3.29}$$

where in addition to satisfy $x_\mu(0) = x_\mu(1)$ as in the case of zero temperature, x_μ should satisfy an additional constraint of periodicity in x_4 direction.

As argued in zero temperature case, taking exponent in the eq.(3.29) as $-S_{\text{eff}}(x)$, then in the weak field limit we get equation of motion as (3.17). A point to note that in eq.(3.29), the case of $n = 0$ has already been evaluated in the zero temperature case. Hence only remaining part is that of $n \neq 0$ which would contribute to finite temperature correction to vacuum decay rate expression. For finding finite temperature Instanton solution, we need to find solution of equation of motion eq.(3.17) where solution is periodic in x_4 direction with period $n\beta$. Such solution to given equation of motion, we have found in the case of scalar.

There are two solutions for $n \in \mathbb{Z}^+$ - Path I^+ and Path II^+ as represented in 2.2. The path I^+ given by solution eq.(2.84) contribute to free energy of the created pair. The path II^+ given by solution eq.(2.88) contributes to the vacuum decay rate expression. There are two solutions for $n \in \mathbb{Z}^-$ - Path I^- and Path II^- as represented in 2.1. The path I^- given by solution eq.(2.77) contribute to free energy of the created pair. The path II^- given by solution eq.(2.81) contributes to the vacuum decay rate expression. As mentioned in the scalar case contribution from II^+ and II^- is same in the vacuum decay rate expression. Hence sum over $n \in \mathbb{Z}$ in eq.(3.29) will be replaced by twice sum over $n \in \mathbb{Z}^+$.

The contribution from exponential terms for the case of constant E case is given by

$$\exp(-S_{\text{eff}}(\bar{x}^{\mathrm{T},II^+}))\cos(eET_0/m^2) \tag{3.30}$$

substituting $S_{\text{eff}}(\bar{x}^{\mathrm{T},II^+})$ from eq.(2.89) and using $T_0 = ma/2 = mR\vartheta/2$ we get

$$\exp\Big(-\frac{m^2}{2eE}\Big[2\pi(p+1) - 2\arcsin\big(\frac{nT_c}{T}\big)\Big] + \frac{nm}{2T}\sqrt{1-\frac{n^2T_c^2}{T^2}}\Big)\cos\Big(\frac{\vartheta}{2}\Big) \tag{3.31}$$

- Electric field parallel to magnetic field:-

  For the case of $\boldsymbol{E} \shortparallel \boldsymbol{B}$ the equation of motion does not change and hence nor the $S_{\text{eff}}(\bar{x}^{\mathrm{T},II^+})$. The contribution from exponential terms for the case of constant $\boldsymbol{E} \shortparallel \boldsymbol{B}$ case is given by

$$\exp(-S_{\text{eff}}(\bar{x}^{\mathrm{T},II^+}))\cos(eET_0/m^2)\cosh(eBT_0/m^2) \tag{3.32}$$

substituting $S_{\text{eff}}(\bar{x}^{\mathrm{T},II^+})$ from eq.(2.89) and using $T_0 = ma/2 = mR\vartheta/2$ we get

$$\exp\Big(-\frac{m^2}{2eE}\Big[2\pi(p+1) - 2\arcsin\big(\frac{nT_c}{T}\big)\Big] + \frac{nm}{2T}\sqrt{1-\frac{n^2T_c^2}{T^2}}\Big)\cos\Big(\frac{\vartheta}{2}\Big)\cosh\Big(\frac{B\vartheta}{2E}\Big) \tag{3.33}$$

3.2.2 Pre-exponential factor at finite temperature

- Electric case:-

  As argued in zero temperature Spinor case, since S_{eff} does not change hence in the weak field limit ($eE << m^2, eB << m^2$) we get $\det'\boldsymbol{M}$ same as in the case of scalar case. Hence using eq.(2.104)

$$\begin{aligned}\mathscr{P}^{\mathrm{E}}_{\mathrm{T},sp} &= -2\mathscr{P}^{\mathrm{E}}_{\mathrm{T},sc} \\ &= -2\cdot(-1)^p\frac{iV_3\beta}{2}\frac{(eE)^2}{(2\pi)^{3/2}(nm\beta)^{1/2}\vartheta^2}\Big[1-\Big(\frac{n\beta eE}{2m}\Big)^2\Big]^{-1/4}\end{aligned} \tag{3.34}$$

  We just need to take into account the extra factor of -2 as that is the only extra factor arises in the pre-exponential factor of spinor as compared to scalar.

- Electric field parallel to magnetic field:-

  For the similar reasons mentioned in $\boldsymbol{E}$ case, the $\det'\boldsymbol{M}$ for spinor $\boldsymbol{E} \shortparallel \boldsymbol{B}$ case does not change as compared to scalar $\boldsymbol{E} \parallel \boldsymbol{B}$ case. Using eq.(2.114),

$$\begin{aligned}\mathscr{P}^{\mathrm{EB}}_{\mathrm{T},sp} &= -2\mathscr{P}^{\mathrm{EB}}_{\mathrm{T},sc}\\ &= -2\cdot(-1)^{p}\frac{iV_3\beta}{4}\frac{e^2EB}{(2\pi)^{3/2}(nm\beta)^{1/2}\vartheta\sinh\left(\frac{\vartheta B}{2E}\right)}\left[1-\left(\frac{n\beta eE}{2m}\right)^2\right]^{-1/4}\end{aligned} \tag{3.35}$$

3.3 Final Result

3.3.1 Zero Temperature

As already mentioned in section 2.1, the Schwinger pair production rate of Spinor in constant electric background is (3.25)

$$\boxed{\Gamma^{\mathrm{E}}_{0,sp} = \sum_{p=1}^{\infty}\frac{e^2E^2}{4\pi^3p^2}\exp\left[-\frac{m^2p\pi}{eE}\right]} \tag{3.36}$$

This result was derived in [70], we derived it using Worldline Instanton formalism.

And for the background of constant electric field parallel to magnetic field is (3.28)

$$\boxed{\Gamma^{\mathrm{EB}}_{0,sp} = \sum_{p=1}^{\infty}\frac{e^2EB\coth(p\pi B/E)}{4\pi^2p}\exp\left[-\frac{m^2p\pi}{eE}\right]} \tag{3.37}$$

which reduces to $\Gamma^{\mathrm{E}}_{0,sp}$ in the $\boldsymbol{B}\to 0$ limit. This result was derived in [17], we derived it using Worldline Instanton formalism.

3.3.2 Finite Temperature

Schwinger pair production rate at finite temperature $\boldsymbol{T}$ in the background of constant electric field $\boldsymbol{E}$ is

$$\Gamma^{\mathrm{E}}_{sp} = \Gamma^{\mathrm{E}}_{0,sp} + \Gamma^{\mathrm{E}}_{\mathrm{T},sp} \tag{3.38}$$

where $\Gamma^{\mathrm{E}}_{\mathrm{T},sp}$ (using eq.(3.31),eq.(3.34) and eq.(2.6))is given by:

$$\boxed{\Gamma^{\mathrm{E}}_{\mathrm{T},sp} = \sum_{p=0}^{\infty}\sum_{n=1}^{n_{max}} 4(-1)^{p+1}\frac{(eE)^2}{(2\pi)^{3/2}(nm\beta)^{1/2}\vartheta^2}\left[1-\left(\frac{n\beta eE}{2m}\right)^2\right]^{-1/4} \exp\left[-\frac{m^2}{2eE}\left[2\pi(p+1)-2\arcsin\left(\frac{nT_c}{T}\right)\right]+\frac{nm}{2T}\sqrt{1-\frac{n^2T_c^2}{T^2}}\right]\cos\left(\frac{\vartheta}{2}\right)} \tag{3.39}$$

where $n_{max} = \lfloor 2R/\beta \rfloor$ and

$$\vartheta = 2\pi(p+1) - \theta_n = 2\pi(p+1) - 2\arcsin\left(\frac{nT_c}{T}\right) \tag{3.40}$$

It is easy to note that $\Gamma^{\mathrm{E}}_{sp} = \Gamma^{\mathrm{E}}_{0,sp}$ for $T = 0$, since for $T < T_c$ there are no thermal corrections. Schwinger pair production rate at finite temperature T in the background of constant electric field E parallel to magnetic field B is

$$\Gamma^{\mathrm{EB}}_{sp} = \Gamma^{\mathrm{EB}}_{0,sp} + \Gamma^{\mathrm{EB}}_{T} \tag{3.41}$$

where $\Gamma^{EB}_{\mathrm{T},sp}$ (using eq.(3.32),eq.(3.35) and eq.(2.6))is given by:

$$\boxed{\Gamma^{\mathrm{EB}}_{\mathrm{T},sp} = \sum_{p=0}^{\infty}\sum_{n=1}^{n_{max}} 2(-1)^{p+1}\frac{e^2EB}{(2\pi)^{3/2}(nm\beta)^{1/2}\vartheta\sinh\left(\frac{\vartheta B}{2E}\right)}\left[1-\left(\frac{n\beta eE}{2m}\right)^2\right]^{-1/4} \exp\left[-\frac{m^2}{2eE}\left[2\pi(p+1)-2\arcsin\left(\frac{nT_c}{T}\right)\right]+\frac{nm}{2T}\sqrt{1-\frac{n^2T_c^2}{T^2}}\right]\cos\left(\frac{\vartheta}{2}\right)\cosh\left(\frac{\vartheta B}{2E}\right)} \tag{3.42}$$

where $n_{max} = \lfloor 2R/\beta \rfloor$ and

$$\vartheta = 2\pi(p+1) - \theta_n = 2\pi(p+1) - 2\arcsin\left(\frac{nT_c}{T}\right) \tag{3.43}$$

In the limit of $B \to 0$, $\Gamma^{\mathrm{EB}}_{sp}$ reduces to Γ^{E}_{sp}. Since in the $B \to 0$ limit

$$\sinh\left(\frac{\vartheta B}{2E}\right) \to \frac{\vartheta B}{2E} \tag{3.44}$$

thus $\Gamma^{\mathrm{EB}}_{\mathrm{T},sp} \to \Gamma^{\mathrm{E}}_{\mathrm{T},sp}$. It is easy to note that $\Gamma^{\mathrm{EB}}_{sp} = \Gamma^{\mathrm{EB}}_{0,sp}$ for $T = 0$, since for $T < T_c$ there are no thermal corrections.

Chapter 4

Millicharged particle

4.1 One Para-photon Model

Millicharged particles can be accommodated in the SM itself, or through kinetic mixing with SM singlet dark sector (henceforth denoted by D). In the simplest model, single $U(1)_D$ massless gauge field A_μ^D is kinetically mixed with $U(1)_Y$ gauge field B_μ, the Lagrangian density for this model is [55]

$$\mathscr{L} \supset \bar{\chi}_{\mathrm{D}} \left(i\gamma^\mu \partial_\mu - e_{\mathrm{D}} \gamma^\mu A_\mu^{\mathrm{D}} - m_\chi \right) \chi_{\mathrm{D}} - \frac{1}{4} A_{\alpha\beta}^{\mathrm{D}} A^{\mathrm{D}\,\alpha\beta} - \frac{\xi}{2} A_{\alpha\beta}^{\mathrm{D}} B^{\alpha\beta} \tag{4.1}$$

where χ_{D} is a Dirac fermion in the dark sector, of mass m_χ, charged under A_α^{D} with a coupling $-e_{\mathrm{D}}$. B_α is the hypercharge $U(1)_{\mathrm{Y}}$ gauge field. ξ is kinetic mixing parameter. Field strengths are defined in the usual way $X_{\alpha\beta} \equiv \partial_\alpha X_\beta - \partial_\beta X_\alpha$.

We make field redefinition $A_\mu^D \to A_\mu^D - \xi B_\mu$

$$\mathscr{L} \supset \bar{\chi}_{\mathrm{D}} \left(i\gamma^\mu \partial_\mu - e_{\mathrm{D}} \gamma^\mu A_\mu^{\mathrm{D}} + \xi e_{\mathrm{D}} \gamma^\mu B_\mu - m_\chi \right) \chi_{\mathrm{D}} - \frac{1}{4} A_{\alpha\beta}^{\mathrm{D}} A^{\mathrm{D}\,\alpha\beta} \tag{4.2}$$

We have dropped the terms containing quadratic order of ξ. As a consequence of field redefinition, the kinetic mixing term has been eliminated and χ_{D} get effectively coupled to B_α with coupling ξe_{D}. Since ξ can be fractional, the coupling can have arbitrary small

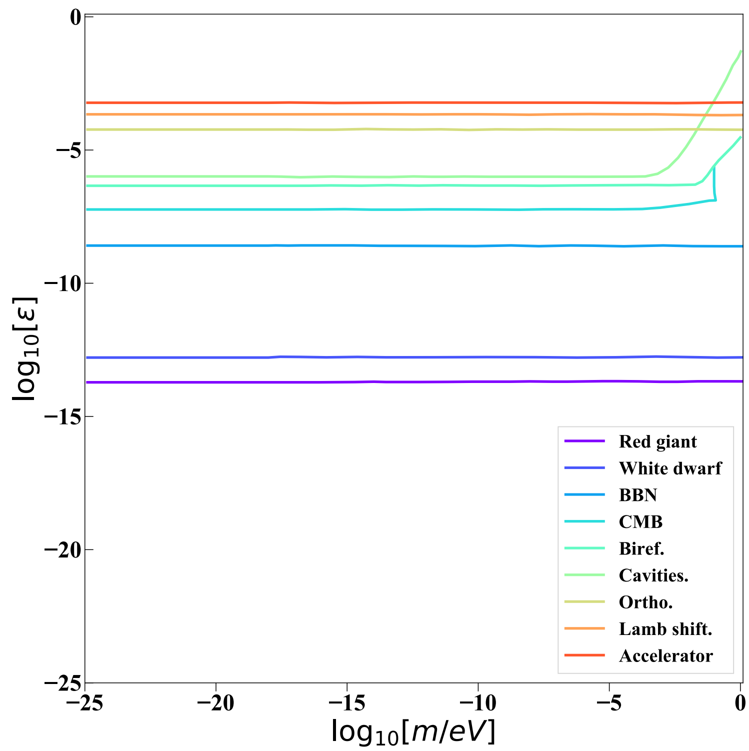

Figure 4.1: This figure summarizes some of the bounds on parameter space of Milli-charged particle

values. After Electro-Weak symmetry breaking, $\chi_{\rm D}$ get coupled to $U(1)_{\rm QED}$ photon with small, fractional electromagnetic charge of magnitude $\xi e_{\rm D}\cos(\theta_w)$ where θ_w is the Standard Model weak mixing angle. Hence ε in units of electric charge becomes

$$\varepsilon \equiv \xi \frac{e_{\rm D}}{e} \cos\theta_{\rm W} \tag{4.3}$$

4.2 Existing Constraints

Many experimental and phenomenological arguments have been proposed in order to put constraints on the parameter space of Milli-charged particles. Direct laboratory searches have been performed in accelerators[71], beam dump experiment at SLAC[72] and Ortho-positronium decays [73]. For ($m_\chi <$ keV) mass range of Millicharged particles the most relevant constraints come from stellar cooling arguments (see Fig.4.2). The stellar energy loss due to the emission of MCP pairs by Plasmon (photon in plasma) decay can put constraints on these particles. For instance, emission of MCP pairs by Plasmon can delay helium flash in red-giants, accelerate the helium-burning stage and cooling of white dwarfs. These constraints exclude $\varepsilon < 10^{-14}$ MCPs [74][75]. But, these constraints are model dependent and can be evaded [76].

4.3 Two Para-photon Model

The two para-photon model can evade the constraints from Red giants and White Dwarfs[76]. The Lagrangian density for the photon part can be written succinctly in the matrix notation as follows:

$$\mathscr{L} = -\frac{1}{4}F^T \mathscr{M}_F F + \frac{1}{2}A^T \mathscr{M}_A A + e\sum_i j_i A_i \tag{4.4}$$

where $A \equiv (A_0, A_1, A_2)^T$ and $F = (F_0, F_1, F_2)^T$. The A_0, A_1, A_2 are interacting fields because interaction term is diagonal in above equation, since only the interaction photon is coupled directly to SM particles. The kinetic matrix $\mathscr{M}_F$ and mass matrix $\mathscr{M}_A$ is given by

$$\mathscr{M}_F = \begin{bmatrix} 1 & \varepsilon & \varepsilon \\ \varepsilon & 1 & 0 \\ \varepsilon & 0 & 1 \end{bmatrix} \qquad \mathscr{M}_A = \begin{bmatrix} m_0^2 & 0 & 0 \\ 0 & m_1^2 & 0 \\ 0 & 0 & m_2^2 \end{bmatrix}$$

The currents $j_0 = 0$, $j_1 = \bar{\chi}_{\mathrm{D}} \gamma_\mu \chi_{\mathrm{D}}$ and $j_2 = -\bar{\chi}_{\mathrm{D}} \gamma_\mu \chi_{\mathrm{D}}$. We have set unit of para-charge equal to unit electric charge e, we also have assigned opposite para-charges w.r.t A_1 and A_2 i.e. coupling with A_1 is taken to be e and that with A_2 be $-e$. We need to make $\mathscr{M}_F$ diagonal such that first term of Lagrangian density will be of form $-F^T F/4$. After this, one needs to diagonalize mass matrix with an unitary transformation that maintains the kinetic part canonical in the propagating field basis $\tilde{A}$. The whole results in $A = U\tilde{A}$ with

$$U = \begin{bmatrix} 1 & \varepsilon \frac{m_1^2}{m_0^2 - m_1^2} & \varepsilon \frac{m_2^2}{m_0^2 - m_2^2} \\ \varepsilon \frac{m_0^2}{m_1^2 - m_0^2} & 1 & 0 \\ \varepsilon \frac{m_0^2}{m_2^2 - m_0^2} & 0 & 1 \end{bmatrix}$$

A point to note that we are working at first order in ε. Now adopting special case of this general model where only one para-photon has mass $m_1 \equiv \mu \neq 0$, and $m_2 = 0$. We observe that under the transformation from interacting fields basis (A) to propagating field basis

$(\tilde{A})$. The last term in equation(4.4) becomes

$$e\bar{\chi}_{\rm D}\gamma_\mu\chi_{\rm D}(A_1^\mu - A_2^\mu) = e\bar{\chi}_{\rm D}\gamma_\mu\chi_{\rm D}(U_{10} - U_{20})\tilde{A}_0^\mu = \varepsilon e\bar{\chi}_{\rm D}\gamma_\mu\chi_{\rm D}\tilde{A}_0^\mu \frac{m_1^2}{m_1^2 - m_0^2} \tag{4.5}$$

In plasma the dispersion relation for photon is

$$k^2 = w_p^2 = \frac{4\pi\alpha n_e}{m_e}$$

where n_e and m_e are density and mass of electrons. The mass of photon is $m_0 = w_p$ in plasma. If $m_0 = w_p >> m_1 = \mu$ then [76]

$$q_\chi(k^2 = w_p^2) \backsimeq \frac{\mu^2}{w_p^2} q_\chi(k^2 = 0) \tag{4.6}$$

for low energy scale of the order of keV i.e. $w_p \approx$ keV, we get a strong decrease in charge of χ in plasma. Thus in vacuum, constraint on ε coming from Red Giants and White Dwarfs are given by $\varepsilon < 10^{-7}$[77].

Chapter 5

Astrophysical Probes on Millicharged Particles from Neutron Stars

5.1 Neutron Stars and Magnetars

Neutron stars are end products of supernova collapse of very massive stars [78, 79]. Radio pulsars and X-ray pulsars are Isolated neutron stars. The latter consists of two groups - soft gamma repeaters (SGR) and anomalous x-ray pulsar (AXP). Radio pulsars are rotationally powered while SGR and AXPs are Magnetically powered. This comes from the observation of short-lived burst activities and persistence emission from the X-ray pulsars, and they are explained under the Magnetar Model[80]. Thus in Magnetar, burst activities and persistence emission is powered by super-strong magnetic field ($O(10^{15})$).

Neutron stars (NS) are rotating objects with high magnetic field which lead to generation of high electric field outside NS. If Lorentz force on particles present on surface exceed the gravitational force, these particles get extracted out and form NS magnetosphere (NSM). NSM rotates with NS upto a distance defined by imaginary surface known as 'Light cylinder'. Inside neutron star magnetosphere, charges reconfigure themselves to nullify electric field induced by Magnetic field, and Lorentz force free condition is maintained. This is the Goldreich-Julian model[81]. The various regions of typical Neutron star are illustrated in Fig.5.1

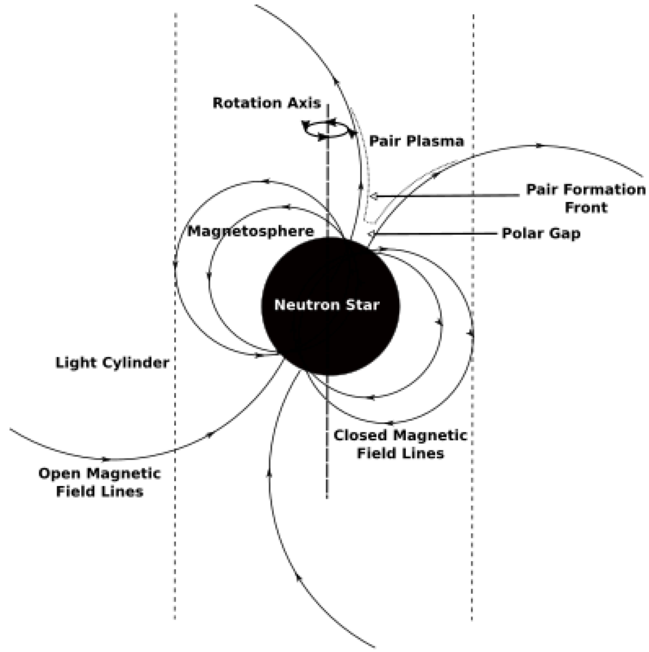

Figure 5.1: A schematic representation of the various relevant NS regions.

The force free state is not maintained throughout the magnetosphere and many model predict the existence of vacuum gap region where the plasma density is low or vanishing. Two vacuum gaps are thought to be present-one just above poles, termed as Polar Gap (PG) and another near the light cylinder, a region between open field lines and closed field lines, termed as Outer gap. In these regions force-free condition is not maintained. In the PG region large electric fields (E_{PG}) parallel to magnetic fields are present, and is given by expression [82]:

$$E_{\rm PG} = \frac{1}{2}\Omega_{\rm NS} B_{\rm NS} R_{\rm NS} \cos^3[\theta] \tag{5.1}$$

Here, $B_{\rm NS}$ is the polar magnetic field on the NS surface, $R_{\rm NS}$ is the NS radius and θ is the star-centered polar angle. Taking representative Magnetar parameter values (denoted 'M') rotation period $\tau_{\rm M} = 10$sec, radius $R_{\rm M} = 10$Km, and $B_{\rm M} = 10^{15}$G, one gets in the MG case $E_{\rm M,PG} = 10^{14}$V/m.

The Polar gap radius is approximately given by

$$R_{\rm PG} \simeq 150\,{\rm m}(\tau_{\rm NS}/{\rm s})^{-\frac{1}{2}} \tag{5.2}$$

where $\tau_{\rm NS}$ is the NS rotation period. Specializing to MGs, with $\tau_{\rm M} = 10\,$s, one obtains

$R_{\text{M,PG}} \simeq 50\,\text{m}$. The pair formation front determines the Polar gap slot width and height. Above the pair formation front region electric fields are shortened out because of the secondary pair plasma gets formed. The typical pair formation front height (distance between pole of NS and starting point of pair formation front see fig.5.1) and polar gap slot width for Magnetar is taken to be 10m [83]. With these dimensions and assuming $|\vec{E}_{\text{M,PG}}|$ is significant in the slot-gap at least all the way upto a height $\mathscr{O}(2R_{\text{NS}})$, we may estimate a relevant PG volume ($\mathscr{V}_{\text{PG}}$); where electric fields are large.

$$\mathscr{V}_{\text{PG}} = 1.46 * 10^{39} m^3 \tag{5.3}$$

5.2 New Constraints on Millicharged Particle

Schwinger pair production (SPP) is a non-perturbative process, i.e. SPP can not be seen at any order in perturbation theory. The signature of non-perturbative behavior can be seen in the decay rate expression for SPP given by Schwinger [2].

$$\Gamma^{E}_{\text{SPP}} = \frac{(eE)^2}{4\pi^3} \exp\left[-\frac{m^2\pi}{eE}\right] \tag{5.4}$$

This equation gives average rate of electron-positron pairs produced per unit volume when external electric field of magnitude E is applied. If the coupling constant (e) is taken to be small, though each term in Taylor expansion of decay rate expression diverges, the expression as a whole converges, signifying non-perturbative behavior.

When the exponent is $O(1)$, the electric field gives the expression for critical electric field strength (E_{cr}), which is the minimum electric field required to produce significant number of pairs. In case of e^+e^-, the $E_{cr} = 10^{18}$V/m. At the time of pair production, electron-positron pair are produced at a distance $l_0 = 2m/eE$ as given by energy conservation.

When electric field is accompanied by parallel magnetic field (B), the decay rate expression modifies. For Spinor electron-positron pair production [84],[85] it is given as

$$\Gamma^{EB}_{\text{SPP}} = \frac{(e^2EB)}{(4\pi^2)} \coth\left[\frac{\pi B}{E}\right] \exp\left[-\frac{m^2\pi}{eE}\right] \tag{5.5}$$

For scalars, apart from overall factor of $1/2$, the $\coth(\pi B/E)$ factor is replaced by $(\sinh(\pi B/E))^{-1}$

factor. Hence, for the values $B_{\rm M} = 10^{15}\,{\rm G}$ and induced $|\vec{E}_{\rm M,PG}| = 10^{14}\,{\rm Vm}^{-1}$ the pair production of scalar particles is suppressed. Hence, the bounds we will derive are only valid for Spinor particles.

5.2.1 Energy-Loss Argument

The rate of energy loss from Magnetar averaged over lifetime of Magnetar $\mathscr{T}_{\rm M}$ is given by

$$\int d\mathscr{V} \left[\frac{d^2\mathscr{E}_{\rm RL}}{dt\, d\mathscr{V}} + \frac{d^2\mathscr{E}^{\chi\bar{\chi}}_{\rm SPP}}{dt\, d\mathscr{V}} \right] \lesssim \int d\mathscr{V} \frac{1}{\mathscr{T}_{\rm M}} \left[\frac{\vec{B}^2_{\rm M}}{2\mu_0} + \frac{\varepsilon_0 \vec{E}^2_{\rm M,PG}}{2} \right]. \tag{5.6}$$

where first term on the LHS is the radiation loss powered by Magnetic field energy. The second term on the LHS quantifies the energy loss due to $\chi_{\rm D}$-SPP. This term is given by

$$\frac{d^2\mathscr{E}^{\chi\bar{\chi}}_{\rm SPP}}{dt\ dV} = \Gamma^{\rm EB}_{\chi\bar{\chi}}\, \varepsilon e |\vec{E}_{\rm M,PG}| l_0 + \Gamma^{\rm EB}_{\chi\bar{\chi}}\, \varepsilon e |\vec{E}'_{\rm M,PG}| (l - l_0)\ . \tag{5.7}$$

Here, $\vec{E}_{\rm M,PG}$ and $\vec{E}'_{\rm M,PG}$ are the average electric field values over the respective distance ranges. The first term in Eq. (5.7) is the energy extracted per unit volume per unit time from the $\vec{E}_{\rm M,PG}$ field for SPP. l_0 is the inter-mCP distance at the instant of SPP. The second term in Eq. (5.7) is the subsequent work that may be done by $\vec{E}'_{\rm M,PG}$ in accelerating one of the $\chi_{\rm D}$ particles out by a distance $l - l_0$.

In (m_χ, ε) regions where inter-mCP dark Coulombic attraction ($F^{\rm Coul.}_{\rm D} \sim e^2_{\rm D}/l^2_o$) exceeds external Lorentz force ($F_{\rm E} \sim \varepsilon e|\vec{E}_{\rm M,PG}|$), no mCPs accelerate the pairs would instead annihilate soon after SPP. Thus, the second term in Eq. (5.7) gives no contribution in these regions and the only energy extracted from the EM field is to initiate $\chi_{\rm D}$-SPP. In other regions where $F_{\rm E} > F^{\rm Coul.}_{\rm D}$, energy is extracted from the EM field both for SPP and to subsequently accelerate mCPs out of the Magnetars polar gap region.

For the Electromagnetic energy stored in the Magnetar, we assume that most of it is within a distance of R_{NS} of neutron star Magnetosphere. The $\int d\mathscr{V}$ can be taken to be $\mathscr{V}_{\rm PG}$, as discussed earlier.

As an estimate of the radiation loss component, we take the average of the persistent quiescent X-ray emissions (PQXR) from the MG catalog [86] for all currently known MG candidates. This gives

$$\left\langle \int d\mathscr{V}\, d^2\mathscr{E}_{\rm RL}/dtd\mathscr{V} \right\rangle_{\rm M}^{\rm PQXR} \;=\; 4.3\times10^{34}\,{\rm ergs\,s^{-1}} \tag{5.8}$$

In regions where $F_{\rm E} > F_{\rm D}^{\rm Coul.}$ and $\chi_{\rm D}$-SPP occurs, one gets from Eq. (5.6) a bound

$$\varepsilon \;\lesssim\; 10^{-12} \quad (\text{for regions with } F_{\rm E} > F_{\rm D}^{\rm Coul.})\,. \tag{5.9}$$

This is obtained taking typical MG values $\tau_{\rm M} = 10\,{\rm s}$, $R_{\rm M} = 10\,{\rm Km}$, $\mathscr{T}_{\rm M} = 10^4\,{\rm yrs}$ and $B_{\rm M} = 10^{15}\,{\rm G}$ and assuming $l = 20\,{\rm Km}$. In regions where $F_{\rm E} < F_{\rm D}^{\rm Coul.}$, the only energy extracted from the EM field is to achieve SPP. In this situation bound is obtained by putting $l = l_0$ in Eq. (5.7). The inter-mCP distance l_0 at the instant of SPP is given by [31]

$$l_0 = \frac{2m_\chi}{\varepsilon e|\vec{E}_{\rm M,PG}|}\,. \tag{5.10}$$

This is valid for both strong coupling and large fields by energy conservation and symmetry. With these considerations, Eq. (5.6) for $F_{\rm E} < F_{\rm D}^{\rm Coul.}$ gives a bound

$$\varepsilon^2\left(\frac{m_\chi}{1\,{\rm eV}}\right) \;\lesssim\; 10^{-16} \quad (\text{for regions with } F_{\rm E} < F_{\rm D}^{\rm Coul.})\,, \tag{5.11}$$

in regions where $\chi_{\rm D}$-SPP is unsuppressed.

Note that these limits only depend on the fact that fermion mCPs have an effective coupling with the $U(1)_{\rm QED}$ photon. Any model dependent charge screening mechanism in plasma is also irrelevant in the the Magnetar vacuum gap regions. We have neglected any inhomogeneities present, which supported by the fact that the mCP de-Broglie wavelength is small and well within the Polar Gap region[87]. In addition we also have $l_0 << 10m$ putting it well within the polar gap region at the time of SPP.

5.2.2 Magnetic Field Evolution Argument

In this subsection we will show how does the $\chi_{\rm D}$-SPP affect the magnetic field evolution and spin down rate of Magnetar. We include Ohmic and Hall drift contribution in the decay of magnetic field [88][89], along with potential $\chi_{\rm D}$-SPP contribution one has for mag-

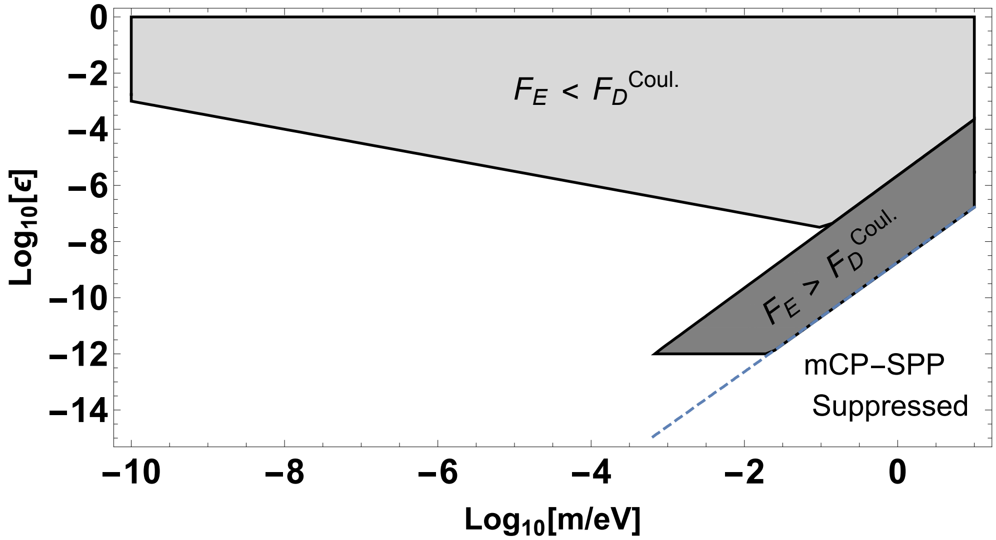

Figure 5.2: Gray and Dark gray region is the excluded region. mCP-SPP suppressed is the region where $E_{cr} > 10^{14}$V/m hence production of mCP pairs is exponentially suppressed.

netic field evolution

$$\frac{dB_{\rm M}(t)}{dt} = -\frac{B_{\rm M}(t)}{\tau_{\rm O}} - \frac{B^2_{\rm M}(t)}{B_{\rm M}(0)\tau_{\rm H}} - \frac{3\varepsilon^3 e^3 \Omega^2_{\rm M}(t) B^2_{\rm M}(t) l}{8\pi^2 R_{\rm M}} \mathscr{V}_{\rm PG} \coth\left[\frac{2\pi}{\Omega_{\rm M}(t) R_{\rm M}}\right] \exp\left[-\frac{2\pi m^2_\chi}{\varepsilon e \Omega_{\rm M}(t) R_{\rm M} B_{\rm M}(t)}\right] . \quad (5.12)$$

contribution from neutron star dynamo, responsible for evolution of magnetic field in the early stages of proto-neutron star formation is assumed to be absent[80]. We have also neglected the Ambipolar diffusion[89]. $B_{\rm M}(0)$ is the initial magnetic field, which we take as 10^{15} G. $\Omega_{\rm M}(t)$ is the MG angular velocity. $\mathscr{V}_{\rm PG}$ as before is the relevant PG volume. For the Ohmic and Hall drift time constants, we take $\tau_{\rm O} = 10^6$ yrs and $\tau_{\rm H} = 10^4$ yrs following typical values from literature [88, 90]. The time constants $\tau_{\rm O}$ and $\tau_{\rm H}$ are complex function of temperature and density, but the relevant behavior has been shown to be captured in these values. Similarly, the $B_{\rm M}(t)$ of the above form qualitatively reproduce the results from more complex magneto-thermal evolution[89]. We will also neglect the effects of toroidal fields, glitches, burst and flare events.

Since for viable (m_χ, ε) values, the $\chi_{\rm D}$-SPP should not overwhelm the conventional $B_{\rm M}(t)$ evolution in the MG. Based on this argument we can out constraint using Eq. (5.12) as follows:

$$\frac{B_{\rm M}(0)}{\tau_{\rm O}}+\frac{B_{\rm M}(0)}{\tau_{\rm H}} > \frac{3\varepsilon^3 e^3\Omega_{\rm M}^2(0)B_{\rm M}^2(0)l}{8\pi^2 R_{\rm M}}\coth\left[\frac{2\pi}{\Omega_{\rm M}(0)R_{\rm M}}\right] \exp\left[-\frac{2\pi m_\chi^2}{\varepsilon e\Omega_{\rm M}(0)R_{\rm M}B_{\rm M}(0)}\right]\mathscr{V}_{\rm PG}\,. \tag{5.13}$$

This gives a constraint

$$\varepsilon < 3.4\times 10^{-12} \quad (\text{for regions with } F_{\rm E} > F_{\rm D}^{\rm Coul.})\,, \tag{5.14}$$

in regions where $F_{\rm E}$ dominates and $\chi_{\rm D}$-SPP occurs. In regions where $F_{\rm D}^{\rm Coul.}$ dominates, we set as before $l = l_0(m_\chi, \varepsilon, B_{\rm M}(0), \Omega_{\rm M}(0))$ in (5.13), where l_0 is given by in Eq.(5.10). For these regions, we have

$$\varepsilon^2\left(\frac{m_\chi}{1\,{\rm eV}}\right) < 6.4\times 10^{-17} \quad (\text{for regions with } F_{\rm E} < F_{\rm D}^{\rm Coul.})\,. \tag{5.15}$$

A point to note that bounds coming from Eqs. (5.6) and (5.13) are comparable. This makes sense since without mCP SPP, the Ohmic and Hall terms lead to $B_{\rm M}$ dissipation, which subsequently power persistent emissions. Thus, our arguments based on MG energetics are related to those based on $B_{\rm M}(t)$ evolution. The complete exclusion regions based on these arguments from Eqs. (5.6) and (5.13) are shown in Fig. 5.2.1. We have assumed $e_{\rm D}\sim e$ for the calculation of l_0.

5.2.3 Effect on Braking Index

The effect of $\chi_{\rm D}$-SPP can be seen in $\Omega_{\rm NS}(t)$ which will be encapsulated in the 'braking-index' of Neutron star. For a relation $\dot{\Omega}_{\rm NS}(t) = -\lambda(t)\Omega_{\rm NS}^b(t)$, the true braking-index ($b_{\rm true}$) is given by

$$b_{\rm true}(t) = \frac{\Omega_{\rm NS}(t)\ddot{\Omega}_{\rm NS}(t)}{\dot{\Omega}_{\rm NS}^2(t)} = b + \frac{\dot{\lambda}(t)\Omega_{\rm NS}(t)}{\lambda(t)\dot{\Omega}_{\rm NS}(t)}\,. \tag{5.16}$$

If $\lambda(t)$ is a constant, one obtains $b_{\rm true} = b$. For instance, a rotating, constant magnetic dipole has $b_{\rm true} = 3$. In general, $b_{\rm true}$ is time dependent as seen from Eq. (5.16).

Assuming a predominantly dipolar magnetic field in the neutron star exterior, the spin-

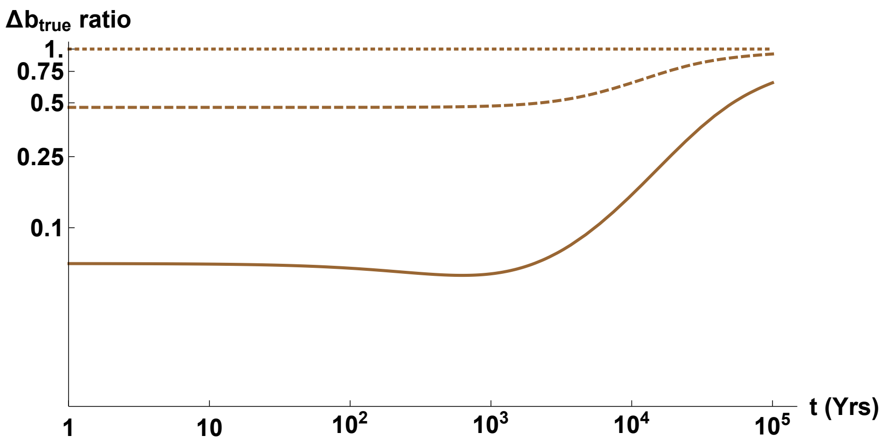

Figure 5.3: The ratio $\Delta b^{\not{\text{SPP}}}_{\text{true}}/\Delta b^{\text{SPP}}_{\text{true}}$ for $M_\chi = 10^{-2}\,\text{eV}$ and $\varepsilon = 10^{-11}$ (solid), 10^{-12} (dashed) and 10^{-13} (dotted).

down due to magnetic-braking torque is given by

$$I_{\text{NS}}\,\dot{\Omega}_{\text{NS}} = -1/6\,\Omega^3_{\text{NS}} B^2_{\text{NS}} R^6_{\text{NS}} \sin^2\alpha \tag{5.17}$$

where I_{NS} is moment of inertia of neutron star and α is the angle between neutron star rotation and magnetic axes. Without loss of generality we take $\alpha = \pi/4$ and neglect the time dependence I_{NS} might have. Specializing to a Magnetar and approximating it to a spinning rigid sphere with $I_{\text{M}} = \frac{2}{5} M_{\text{M}} R^2_{\text{M}}$, we get

$$\dot{\Omega}_{\text{M}}(t) = -\frac{5}{24}\frac{R^4_{\text{M}}}{M_{\text{M}}} B^2_{\text{M}}(t)\Omega^3_{\text{M}}(t)\,. \tag{5.18}$$

We solve the coupled differential equations, Eqs. (5.12) and (5.18), for $B_{\text{M}}(t)$ and $\Omega_{\text{M}}(t)$ over a time-scale $[1.0,\, 1\times 10^5]\,\text{yrs}$. Based on the solution we may calculate $b_{\text{true}}(t)$ for various (m_χ, ε) values.

Define the deviation of $b_{\text{true}}(t)$ from the pure magnetic dipole braking index as $\Delta b_{\text{true}}(t) \equiv b_{\text{true}}(t) - 3$. The ratio of this quantity, without χ_{D}-SPP ($\Delta b^{\not{\text{SPP}}}_{\text{true}}$) to that with χ_{D}-SPP ($\Delta b^{\text{SPP}}_{\text{true}}$), is shown in Fig. 5.2.2. The curves are for parametric values $\varepsilon = \{10^{-11}, 10^{-12}, 10^{-13}\}$ and $m_\chi = 10^{-2}\,\text{eV}$. For these values $F_{\text{E}} > F^{\text{Coul.}}_{\text{D}}$. The ratios $\Delta b^{\not{\text{SPP}}}_{\text{true}}/\Delta b^{\text{SPP}}_{\text{true}}$ differ from unity and for large ε values show appreciable time evolution. This therefore provides a further avenue where χ_{D}-SPP effects may be probed.

Chapter 6

Conclusion and Outlook

Millicharged particles, a viable dark matter candidate, are intriguing because of their fractional charges. The most stringent condition till now was from stellar cooling arguments. But these constraints as was shown are model dependent and constraints in vacuum on ε can be brought down to 10^{-7} in sub-KeV mass range.

In this thesis, we have obtained a novel, model-independent constraints from the non-perturbative production of the Millicharged particles in Magnetar environment. The constraint from the energy-loss argument for the region of $m_\chi - \varepsilon$ parameter space where $F_E > F_D^{Coul}$ are $\varepsilon < 10^{-12}$ and $\varepsilon^2 \left(\frac{m_\chi}{1\,\mathrm{eV}}\right) \lesssim 10^{-16}$ for $F_E < F_D^{Coul}$ region. Approximately similar bounds are obtained from the magnetic field evolution argument. This is expected as Schwinger pair production of Millicharged particle was absent, the Ohmic and Hall term led to the B_M dissipation which power the persistent emission. We have shown that depending on the ε values a significant change is seen in the braking index of Magnetar. We have neglected the Magneto-thermal evolution of time constants. We also neglected the effects of toroidal components, glitches, flares which would be necessary for the more complete modeling. The basic principle is that of adding χ_{D}-SPP term in the $B_M(t)$ evolution.

The idea of SPP of Millicharged particles can be extended to Milli-magnetically charged particles (mMCP). We are trying to find the effect of SPP of mMCPs on the braking index of Magnetar and on the continuous gravitational waves produced from Neutron star.

In this thesis we have shown using the Worldline Instanton formalism the previously obtained results for vacuum decay rate for Scalar QED and QED vacuum. We verified the results for zero temperature, constant Electric case and constant Electric Field parallel to Magnetic Field case for both scalar and Spinor.

Worldline formalism has an easy generalization to finite temperature case. We verified the previously obtained result for scalar QED vacuum decay rate in constant Electric field at finite temperature . We obtained a new result for scalar QED in constant Electric field parallel to Magnetic field background. This result indeed reduced to pure electric field result under $\boldsymbol{B} = 0$ limit. We obtained an analytical expression for Spinor QED vacuum decay rate at non-zero temperature in pure Electric and $\boldsymbol{E} \parallel \boldsymbol{B}$ field.

We have assumed a constant Electric field and constant $\boldsymbol{E} \parallel \boldsymbol{B}$ field configuration. There are many ways one can extend this result to make them practically relevant. It was shown at zero temperature that inhomogeneities in Electric and Magnetic field can enhance pair production rate. Analytical formula for the inhomogeneous field configuration at finite temperature would be a test of whether this enhancement holds at non-zero temperature. Calculating pair production rates for spatial and temporal inhomogeneous electric and magnetic field would give us a way to test this non-perturbative phenomenon at future laser facilities. In our calculation we have made an assumption of weak field and weak coupling. It would be a theoretical challenge to see whether this formula holds true for strong field like in the case of zero temperature and how can one account for strong coupling in the formalism.

Appendices

6.1 Morse Analysis

In this section, we will show how the factor of $(-1)^p$ also termed as Morse index of the classical path appears in the pre-exponential factors. The caustic is defines as a envelope of trajectories obtained by fixing $x_\mu(0)$ and varying $\dot{x}_\mu(0)$. A focal point of the classical path is defined as contact point between path and caustic surface. The crux of Morse theory is that the number of negative eigenvalues of the second variation operator about the given classical path equals the number of focal points strictly between the end points counted with their multiplicity. This number assigns Morse Index to path. In reverse, if we can find the Morse index of the path the number of negative eigenvalues can be evaluated. This information is crucial as it will be determining point to distinguish between two finite temperature Instanton solution.

In practice, the Morse index is determined by calculating the number of times eigenvalues of matrix η vanishes strictly between the endpoints. This would give the number of negative eigenvalues of operator L. In order, to calculate total number of negative eigenvalues of M, we need to take into account the extra negative eigenvalue coming from the non-local part of eq.(2.91). As we found in finite temperature case the non-local part gave extra negative eigenvalue only for the case of larger paths and not for the smaller path.

The η matrix we found for the case constant Electric field case has following Eigenvalues:

$$[u, u, i(-1+\cos(\vartheta u) - i\sin(\vartheta u)), -i(-1+\cos(\vartheta u) + i\sin(\vartheta u))] \tag{6.1}$$

The first two eigenvalues will not vanish for $0 < u < 1$. Whenever the third eigenvalue vanish, fourth one will too. Since for the third eigenvalue to be zero both real and imaginary part must vanish simultaneously, hence making fourth eigenvalue to vanish. The third eigenvalue is zero for following u values strictly between 0 and 1.

$$u = \frac{2n\pi}{2\pi(p+1) - \theta_n} \quad n \in 1, 2, \cdots, p \tag{6.2}$$

Hence, the number of negative eigenvalues for L are $2p$. Hence, for the larger paths total number of negative eigenvalues are $2p+1$. It can easily be seen that for small paths total number of negative eigenvalues will be $2p$ only the coming from matrix L. Hence, for the both paths the factor of $e^{-i2\pi p/2} = (-1)^p$ must be taken into account[32],[69]. One must note that even if the Morse index for the longer path is $2p+1$, the contribution for the extra negative eigenvalue coming from non-local part is already accounted for by i factor in the pre-exponential factor. For the case of constant $E \parallel B$ case the conclusions, as mentioned above, will not change. As the extra eigenvalues appearing for this case will not be zero except at the endpoints of the path.

Bibliography

[1] W. Heisenberg and H. Euler. Folgerungen aus der diracschen theorie des positrons. Zeitschrift für Physik, 98(11):714–732, Nov 1936.

[2] Julian Schwinger. On gauge invariance and vacuum polarization. Phys. Rev., 82:664–679, Jun 1951.

[3] GERALD V. DUNNE. The heisenberg–euler effective action: 75 years on. International Journal of Modern Physics A, 27(15):1260004, 2012.

[4] S. W. Hawking. Black hole explosions. Nature, 248:30–31, 1974.

[5] Leonard Parker. Quantized fields and particle creation in expanding universes. i. Phys. Rev., 183:1057–1068, Jul 1969.

[6] A. Casher, H. Neuberger, and S. Nussinov. Chromoelectric-flux-tube model of particle production. Phys. Rev. D, 20:179–188, Jul 1979.

[7] Dmitri Kharzeev and Kirill Tuchin. From color glass condensate to quark–gluon plasma through the event horizon. Nuclear Physics A, 753(3):316 – 334, 2005.

[8] A. Di Piazza, C. Muller, K. Z. Hatsagortsyan, and C. H. Keitel. Extremely high-intensity laser interactions with fundamental quantum systems. Rev. Mod. Phys., 84:1177, 2012.

[9] G. V. Dunne. New strong-field qed effects at extreme light infrastructure. The European Physical Journal D, 55(2):327, Feb 2009.

[10] E. Brezin and C. Itzykson. Pair production in vacuum by an alternating field. Phys. Rev. D, 2:1191–1199, Oct 1970.

[11] Joakim Hallin and Per Liljenberg. Fermionic and bosonic pair creation in an external electric field at finite temperature using the functional schrödinger representation. Phys. Rev. D, 52:1150–1164, Jul 1995.

[12] H.M. Fried and R.P. Woodard. The one loop effective action of qed for a general class of electric fields. Physics Letters B, 524(1):233 – 239, 2002.

[13] J. Avan, H. M. Fried, and Y. Gabellini. Nontrivial generalizations of the schwinger pair production result. Phys. Rev. D, 67:016003, Jan 2003.

[14] S. A. Smolyansky, G. Ropke, S. M. Schmidt, D. Blaschke, V. D. Toneev, and A. V. Prozorkevich. Dynamical derivation of a quantum kinetic equation for particle production in the Schwinger mechanism. 1997.

[15] S. M. Schmidt, D. Blaschke, G. Ropke, S. A. Smolyansky, A. V. Prozorkevich, and V. D. Toneev. A Quantum kinetic equation for particle production in the Schwinger mechanism. Int. J. Mod. Phys., E7:709–722, 1998.

[16] Gerald V. Dunne and Christian Schubert. Worldline instantons and pair production in inhomogenous fields. Phys. Rev. D, 72:105004, Nov 2005.

[17] Sang Pyo Kim and Don N. Page. Schwinger pair production in electric and magnetic fields. Phys. Rev. D, 73:065020, Mar 2006.

[18] Gerald V. Dunne and Theodore M. Hall. Borel summation of the derivative expansion and effective actions. Phys. Rev. D, 60:065002, Aug 1999.

[19] Holger Gies and Klaus Klingmuller. Pair production in inhomogeneous fields. Phys. Rev., D72:065001, 2005.

[20] Sang Pyo Kim, Hyun Kyu Lee, and Yongsung Yoon. Effective action of qed in electric field backgrounds. Phys. Rev. D, 78:105013, Nov 2008.

[21] Walter Dittrich. Effective lagrangians at finite temperature. Phys. Rev. D, 19:2385–2390, Apr 1979.

[22] M. Loewe and J. C. Rojas. Thermal effects and the effective action of quantum electrodynamics. Phys. Rev. D, 46:2689–2694, Sep 1992.

[23] Per Elmfors and Bo-Sture Skagerstam. Electromagnetic fields in a thermal background. Physics Letters B, 348(1):141 – 148, 1995.

[24] Avijit K. Ganguly, Predhiman K. Kaw, and Jitendra C. Parikh. Thermal tunneling of $q\bar{q}$ pairs in a-a collisions. Phys. Rev. C, 51:2091–2094, Apr 1995.

[25] Holger Gies. Qed effective action at finite temperature. Phys. Rev. D, 60:105002, Oct 1999.

[26] Sang Pyo Kim, Hyun Kyu Lee, and Yongsung Yoon. Nonperturbative QED Effective Action at Finite Temperature. Phys. Rev., D82:025016, 2010.

[27] Leandro Medina and Michael C. Ogilvie. Schwinger pair production at finite temperature. Phys. Rev. D, 95:056006, Mar 2017.

[28] Oliver Gould and Arttu Rajantie. Thermal schwinger pair production at arbitrary coupling. Phys. Rev. D, 96:076002, Oct 2017.

[29] Zvi Bern and David A. Kosower. The computation of loop amplitudes in gauge theories. Nuclear Physics B, 379(3):451 – 561, 1992.

[30] Matthew J. Strassler. Field theory without feynman diagrams: One-loop effective actions. Nuclear Physics B, 385(1):145 – 184, 1992.

[31] Ian K. Affleck, Orlando Alvarez, and Nicholas S. Manton. Pair production at strong coupling in weak external fields. Nuclear Physics B, 197(3):509 – 519, 1982.

[32] Gerald V. Dunne, Qing-hai Wang, Holger Gies, and Christian Schubert. Worldline instantons. II. The Fluctuation prefactor. Phys. Rev., D73:065028, 2006.

[33] F. Zwicky. Die Rotverschiebung von extragalaktischen Nebeln. Helvetica Physica Acta, 6:110–127, 1933.

[34] V. C. Rubin, N. Thonnard, and W. K. Ford, Jr. Extended rotation curves of high-luminosity spiral galaxies. IV - Systematic dynamical properties, SA through SC. apjl, 225:L107–L111, November 1978.

[35] J. P. Ostriker and P. J. E. Peebles. A Numerical Study of the Stability of Flattened Galaxies: or, can Cold Galaxies Survive? apj, 186:467–480, December 1973.

[36] D. Fabricant, M. Lecar, and P. Gorenstein. X-ray measurements of the mass of M87. apj, 241:552–560, October 1980.

[37] Richard Massey, Thomas Kitching, and Johan Richard. The dark matter of gravitational lensing. Rept. Prog. Phys., 73:086901, 2010.

[38] Joel R. Primack. Dark matter and structure formation. In Midrasha Mathematicae in Jerusalem: Winter School in Dynamical Systems Jerusalem, Israel, January 12-17, 1997, 1997.

[39] Karsten Jedamzik and Maxim Pospelov. Big Bang Nucleosynthesis and Particle Dark Matter. New J. Phys., 11:105028, 2009.

[40] M. Milgrom. A modification of the Newtonian dynamics as a possible alternative to the hidden mass hypothesis. apj, 270:365–370, July 1983.

[41] Jacob D. Bekenstein. Relativistic gravitation theory for the MOND paradigm. Phys. Rev., D70:083509, 2004. [Erratum: Phys. Rev.D71,069901(2005)].

[42] J. E. Felten. Milgrom's revision of Newton's laws - Dynamical and cosmological consequences. apj, 286:3–6, November 1984.

[43] B. Paczynski. Gravitational microlensing by the galactic halo. apj, 304:1–5, May 1986.

[44] C. Alcock et al. The MACHO project: Microlensing results from 5.7 years of LMC observations. Astrophys. J., 542:281–307, 2000.

[45] B. J. Carr, Kazunori Kohri, Yuuiti Sendouda, and Jun'ichi Yokoyama. New cosmological constraints on primordial black holes. Phys. Rev., D81:104019, 2010.

[46] Bernard Carr, Florian Kuhnel, and Marit Sandstad. Primordial Black Holes as Dark Matter. Phys. Rev., D94(8):083504, 2016.

[47] K. N. Abazajian et al. Light Sterile Neutrinos: A White Paper. 2012.

[48] Alexey Boyarsky, Oleg Ruchayskiy, and Mikhail Shaposhnikov. The Role of sterile neutrinos in cosmology and astrophysics. Ann. Rev. Nucl. Part. Sci., 59:191–214, 2009.

[49] Teresa Marrodán Undagoitia and Ludwig Rauch. Dark matter direct-detection experiments. J. Phys., G43(1):013001, 2016.

[50] Leszek Roszkowski, Enrico Maria Sessolo, and Sebastian Trojanowski. WIMP dark matter candidates and searches - current issues and future prospects. 2017.

[51] Vadim Kuzmin and Igor Tkachev. Ultrahigh-energy cosmic rays, superheavy long living particles, and matter creation after inflation. JETP Lett., 68:271–275, 1998. [Pisma Zh. Eksp. Teor. Fiz.68,255(1998)].

[52] Daniel J. H. Chung, Edward W. Kolb, and Antonio Riotto. Superheavy dark matter. Phys. Rev., D59:023501, 1999.

[53] Fundamental Physics at the Intensity Frontier, 2012.

[54] Joerg Jaeckel and Andreas Ringwald. The Low-Energy Frontier of Particle Physics. Ann. Rev. Nucl. Part. Sci., 60:405–437, 2010.

[55] Bob Holdom. Searching for ε Charges and a New U(1). Phys. Lett., B178:65–70, 1986.

[56] S. A. Abel and B. W. Schofield. Brane anti-brane kinetic mixing, millicharged particles and SUSY breaking. Nucl. Phys., B685:150–170, 2004.

[57] S. A. Abel, M. D. Goodsell, J. Jaeckel, V. V. Khoze, and A. Ringwald. Kinetic Mixing of the Photon with Hidden U(1)s in String Phenomenology. JHEP, 07:124, 2008.

[58] G. Aldazabal, Luis E. Ibanez, F. Quevedo, and A. M. Uranga. D-branes at singularities: A Bottom up approach to the string embedding of the standard model. JHEP, 08:002, 2000.

[59] Brian Batell and Tony Gherghetta. Localized U(1) gauge fields, millicharged particles, and holography. Phys. Rev., D73:045016, 2006.

[60] E. Zavattini et al. Experimental observation of optical rotation generated in vacuum by a magnetic field. Phys. Rev. Lett., 96:110406, 2006. [Erratum: Phys. Rev. Lett.99,129901(2007)].

[61] Christian Schubert. Perturbative quantum field theory in the string inspired formalism. Phys. Rept., 355:73–234, 2001.

[62] Ian K. Affleck, Orlando Alvarez, and Nicholas S. Manton. Pair production at strong coupling in weak external fields. Nuclear Physics B, 197(3):509 – 519, 1982.

[63] Remo Ruffini, Gregory Vereshchagin, and She-Sheng Xue. Electron-positron pairs in physics and astrophysics: from heavy nuclei to black holes. Phys. Rept., 487:1–140, 2010.

[64] I. S. Gradshteyn and I. M. Ryzhik. Table of integrals, series, and products. Elsevier/Academic Press, Amsterdam, seventh edition, 2007. Translated from the Russian, Translation edited and with a preface by Alan Jeffrey and Daniel Zwillinger, With one CD-ROM (Windows, Macintosh and UNIX).

[65] Curtis G. Callan and Sidney Coleman. Fate of the false vacuum. ii. first quantum corrections. Phys. Rev. D, 16:1762–1768, Sep 1977.

[66] Julian Schwinger. On gauge invariance and vacuum polarization. Phys. Rev., 82:664–679, Jun 1951.

[67] D. G. C. McKeon and A. Rebhan. Thermal green's functions from quantum-mechanical path integrals. Phys. Rev. D, 47:5487–5493, Jun 1993.

[68] Erick J. Weinberg. Classical solutions in quantum field theory. Cambridge Monographs on Mathematical Physics. Cambridge University Press, 2015.

[69] S Levit and U Smilansky. A new approach to gaussian path integrals and the evaluation of the semiclassical propagator. Annals of Physics, 103(1):198 – 207, 1977.

[70] Sang Pyo Kim and Don N. Page. Schwinger pair production via instantons in a strong electric field. Phys. Rev., D65:105002, 2002.

[71] S. Davidson, B. Campbell, and D. Bailey. Limits on particles of small electric charge. Phys. Rev. D, 43:2314–2321, Apr 1991.

[72] A. A. Prinz et al. Search for millicharged particles at SLAC. Phys. Rev. Lett., 81:1175–1178, 1998.

[73] A. Badertscher, P. Crivelli, W. Fetscher, U. Gendotti, S. Gninenko, V. Postoev, A. Rubbia, V. Samoylenko, and D. Sillou. An Improved Limit on Invisible Decays of Positronium. Phys. Rev., D75:032004, 2007.

[74] Sacha Davidson, Steen Hannestad, and Georg Raffelt. Updated bounds on millicharged particles. JHEP, 05:003, 2000.

[75] Sacha Davidson and Michael Peskin. Astrophysical bounds on millicharged particles in models with a paraphoton. Phys. Rev. D, 49:2114–2117, Feb 1994.

[76] Eduard Masso and Javier Redondo. Compatibility of CAST search with axion-like interpretation of PVLAS results. Phys. Rev. Lett., 97:151802, 2006.

[77] Steven A. Abel, Joerg Jaeckel, Valentin V. Khoze, and Andreas Ringwald. Illuminating the Hidden Sector of String Theory by Shining Light through a Magnetic Field. Phys. Lett., B666:66–70, 2008.

[78] W. Baade and F. Zwicky. Cosmic rays from super-novae. Proceedings of the National Academy of Sciences, 20(5):259–263, 1934.

[79] W. Baade and F. Zwicky. On super-novae. Proceedings of the National Academy of Sciences, 20(5):254–259, 1934.

[80] R. C. Duncan and C. Thompson. Formation of very strongly magnetized neutron stars - Implications for gamma-ray bursts. apjl, 392:L9–L13, June 1992.

[81] P. Goldreich and W. H. Julian. Pulsar Electrodynamics. apj, 157:869, August 1969.

[82] D. R. Lorimer and M. Kramer. Handbook of Pulsar Astronomy. October 2012.

[83] Alice K. Harding and Alexander G. Muslimov. Particle acceleration zones above pulsar polar caps: electron and positron pair formation fronts. Astrophys. J., 508:328, 1998.

[84] GERALD V. DUNNE. HEISENBERG EULER EFFECTIVE LAGRANGIANS: BASICS AND EXTENSIONS, pages 445–522. WORLD SCIENTIFIC, 2012.

[85] Sang Pyo Kim and Don N. Page. Schwinger pair production in electric and magnetic fields. Phys. Rev. D, 73:065020, Mar 2006.

[86] S. A. Olausen and V. M. Kaspi. The mcgill magnetar catalog. The Astrophysical Journal Supplement Series, 212(1):6, 2014.

[87] V. I. Ritus. Effective Lagrange function of intense electromagnetic field in QED. In Frontier tests of QED and physics of the vacuum. Proceedings, Workshop, Sandansky, Bulgaria, June 9-15, 1998, pages 11–28, 1998.

[88] P. Goldreich and A. Reisenegger. Magnetic field decay in isolated neutron stars. apj, 395:250–258, August 1992.

[89] K. Glampedakis, D. I. Jones, and L. Samuelsson. Ambipolar diffusion in superfluid neutron stars. Monthly Notices of the Royal Astronomical Society, 413(3):2021–2030, 2011.

[90] Deborah N. Aguilera, Jose A. Pons, and Juan A. Miralles. 2D Cooling of Magnetized Neutron Stars. Astron. Astrophys., 486:255–271, 2008.